The lithosphere–asthenosphere system beneath Ireland from integrated geophysical–petrological modeling — I: Observations, 1D and 2D hypothesis testing and modeling

Alan G. Jones [a],[*], Juan Carlos Afonso [b], Javier Fullea [a],[1], Farshad Salajegheh [b]

[a] Dublin Institute for Advanced Studies, 5 Merrion Square, Dublin 2, Ireland
[b] Australian Research Council Centre of Excellence for Core to Crust Fluid Systems/GEMOC, Department of Earth and Planetary Sciences, Macquarie University, North Ryde, NSW 2109, Australia

ARTICLE INFO

ABSTRACT

Modeling the continental lithosphere's physical properties, especially its depth extent, must be done within a self-consistent petrological–geophysical framework; modeling using only one or two data types may easily lead to inconsistencies and erroneous interpretations. Using the LitMod approach for hypothesis testing and first-order modeling, we show how assumptions made about crustal information and the probable compositions of the lithospheric and sub-lithospheric mantle affect particular observables, particularly especially surface topographic elevation. The critical crustal parameter is density, leading to ca. 600 m error in topography for 50 kg m^{-3} imprecision. The next key parameter is crustal thickness, and uncertainties in its definition lead to around ca. 4 km uncertainty in LAB for every 1 km of variation in Moho depth. Possible errors in the other assumed crustal parameters introduce a few kilometers of uncertainty in the depth to the LAB.

We use Ireland as a natural laboratory to demonstrate the approach. From first-order arguments and given reasonable assumptions, a topographic elevation in the range of 50–100 m, which is the average across Ireland, requires that the lithosphere–asthenosphere boundary (LAB) beneath most of Ireland must lie in the range 90–115 km. A somewhat shallower (to 85 km) LAB is permitted, but the crust must be thinned (<29 km) to compensate.

The observations, especially topography, are inconsistent with suggestions, based on interpretation of S-to-P receiver functions, that the LAB thins from 85 km in southern Ireland to 55 km in central northern Ireland over a distance of <150 km. Such a thin lithosphere would result in over 1000 m of uplift, and such rapid thinning by 30 km over less than 150 km would yield significant north–south variations in topographic elevation, Bouguer anomaly, and geoid height, none of which are observed. Even juxtaposing the most extreme probable depleted composition for the lithospheric mantle beneath southern Ireland against the most extreme fertile composition beneath northern Ireland only allows some 20 km of LAB variation; any further variations would produce effects that are well beyond those observed.

One model that satisfies almost all the extant data to first order includes a spinel-peridotite upper lithospheric mantle layer to 85 km in southern Ireland and to 55 km in northern Ireland, thinning over a lateral distance of 150 km. Below this in southern Ireland is a garnet peridotite layer extending down to 115 km, and in northern Ireland a refertilized layer down to 95 km. The mid-lithospheric chemical discontinuity (MLD) at the base of the Spinel Peridotite zone may explain the observed discontinuity in S-to-P (Sp) receiver functions.

© 2013 Elsevier B.V. All rights reserved.

1. Introduction

Geophysical observations related to the deep structure of the Earth are rarely interpreted in a holistic, integrated manner. Most commonly only one data type is modeled and interpreted; this is particularly the case with seismic data, even to the extent that interpretations of two types of seismic data commonly appear to be mutually contradictory. On rare occasions, two types of data are interpreted together, usually in a qualitative sense. Some formal quantitative joint inversion approaches exist, mostly stochastic in nature, for lithospheric-scale problems (e.g., Bodin et al., 2012; Julia et al., 2000; Kozlovskaya et al., 2008; Li et al., 2008; Moorkamp et al., 2007, 2010; Roux et al., 2011; Shen et al., 2013; Sosa et al., 2013), but these can result in models that are not petrologically/geochemically plausible and/or are not consistent with other observations.

We are surely beyond the times when single geophysical datasets can be modeled and interpreted in blissful ignorance of the others,

* Corresponding author. Tel.: +353 1 653 5147x200.
  E-mail address: alan@cp.dias.ie (A.G. Jones).
[1] Now at: Institute of Geosciences (CSIC, UCM), ES-28040 Madrid, Spain

especially given the availability of constraining data at all locations, such as surface topography and geoid height, and at most locations, such as Bouguer anomalies, gravity gradients, and surface heat flow. The Earth is a single physico-chemical system, ultimately characterized by its chemical composition (including fluids), temperature and pressure at every point in the subsurface. Those parameters can be used to derive a self-consistent set of geophysical observables that can in turn be interrogated for the ranges in causative composition, temperature, pressure and fluid content. In this context, several integrated modeling/inversion approaches have become available in recent years (Afonso et al., 2008, 2013a, 2013b; Fullea et al., 2009, 2011; Khan et al., 2006, 2008, 2009, 2011).

In this paper, we will use first-principle arguments to demonstrate the constraints possible on lithospheric structure when data are interpreted within a self-consistent petrological–geophysical framework. We will use a step-by-step approach, starting with the most simple possible models (one-dimension, 1D, with a simple crust) and introducing more complexity as required to fit the various observations. Our final two-dimensional (2D) model has a laterally-varying crust and a lithospheric mantle comprised of three distinct bodies of differing chemistry. Still further complexity is considered in the companion paper by Fullea et al. (2014-this issue), which fits all of the data with a detailed three-dimensional (3D) model.

We take Ireland as our demonstration natural laboratory, and deduce the allowable lithospheric thickness of Ireland given knowledge of its topography, geoid height, Bouguer anomalies, crustal structure and thickness. We make reasonable choices of chemical compositions for its lithospheric mantle, and accept prior suggestions that the lithosphere beneath northern Ireland was affected by magmatism. The tool that we use for our examination is the LitMod software (Afonso et al., 2008), an integrated geophysical–petrological modeling framework that simultaneously solves the equations for heat transfer, thermodynamic, rheological, geopotential, and isostasy.

We focus in particular on the possibility of a generally thin lithosphere beneath Ireland, and of significant (30 km) lithospheric thinning from south to north across Ireland. These suggestions were made on the basis of an S-to-P receiver function study by Landes et al. (2007), and were later incorporated into the interpretation of the P-wave traveltime tomography model by Wawerzinek et al. (2008). P-wave teleseismic tomographic modeling also has been interpreted in terms of thinned lithosphere in northern Ireland (Al-Kindi et al., 2003; Arrowsmith et al., 2005). All of these studies were taken to lend support to the prior suggestion by Kirstein and Timmerman (2000), based on helium isotopes, that the lower lithosphere across northern Ireland was eradicated at ca. 43 Ma as a consequence of a putative proto-Icelandic plume beneath northern Ireland.

In this paper we concentrate on the lithospheric variation beneath the region covered by the Landes et al. (2007) study, namely from the south coast of Ireland to about 54.5°N. There are far fewer data further north, and what data exist are either contentious (Moho depth) or anomalous (surface heat flow) or both. We demonstrate to first order, in both one dimension (1D) and two dimensions (2D), that to fit simultaneously the observed topography, geoid height, Bouguer anomalies, and surface heat flow, Ireland's lithospheric mantle can be no thinner than around 85 km, and conversely nowhere deeper than around 120 km, with the most likely average value being around 105 km. This value is broadly consistent with regional-scale modeling of the lithosphere–asthenosphere boundary (LAB) in NW Europe from thermal considerations (Hamza and Vieira, 2012) and with much earlier work that suggested an LAB beneath Ireland in the range of 110–190 km from a surface wave study (Clark and Stuart, 1981) and an LAB at 106 km derived by modeling events from distant earthquakes and a Chinese nuclear test (Masson et al., 1999).

A companion paper (Fullea et al., 2014-this issue) undertakes a more detailed 3D modeling of the available data for Ireland (elevation, gravity and geoid anomalies, gravity gradients, surface heat flow and

composition from mantle xenolith), using the LitMod3D approach of Fullea et al. (2009), to explore the tectonic setting of the whole island and surrounding offshore areas. In particular, Fullea et al. (2014-this issue) consider the surface heat flow and gravity effects of known granitic bodies in order to match the lateral variation of observations, whereas herein their effects are not considered.

2. Tectonic setting

The tectonic setting of Ireland is dominated by its straddling of the Caledonian Iapetus Suture Zone (ISZ) that similarly divides the island of Newfoundland in two. The understanding of faunal differences between these two terranes was key to the development of plate tectonic theory with Tuzo Wilson's iconic 1966 paper (Wilson, 1966). The Iapetus Ocean, estimated to have been some 5000 km in width, closed in a zipper-like fashion from east to west (present day coordinates) bringing together Laurentia and Avalonia (Chew and Stillman, 2009). The suture has been well studied geologically in Scotland and Newfoundland, where exposure is excellent, but due to poor exposure information about the suture in Ireland comes primarily from geophysics and geochemistry.

Various active and passive seismic experiments have been conducted in Ireland, particularly over the Irish segment of the ISZ, over the last three decades. These include the 1982 Irish Caledonian Suture Seismic (refraction) Project (ICSSP, Jacob et al., 1985), the 1985 Caledonian Onshore–Offshore Lithospheric (refraction) Experiment (COOLE, Lowe and Jacob, 1989), and the 1996 Variscan Network (VARNET) refraction project (Landes et al., 2000, 2003; Masson et al., 1998, 1999), as well as two teleseismic projects, the 2002–2005 Irish Seismic Lithosphere Experiment (ISLE; Do et al., 2006; Landes et al., 2006) and the 2006–2012 Irish Seismological Upper Mantle Experiment (ISUME; Polat et al., 2012). These have been complemented by two magnetotelluric surveys, the Irish Magnetotelluric Profile in the late 1980s (Brown and Whelan, 1995; Whelan et al., 1990), and the Irish Magnetotelluric Lithospheric Experiment ISLE-MT in the mid-2000s (Rao et al., 2007). All of these experiments showed strong crustal anomalies associated with the ISZ, but weak to absent lithospheric structures.

More recently, helium-isotope information gleaned from spinel pyroxenites from the mid-Eocene (42 Ma) xenolith-bearing alkaline Inver dyke in Donegal, NW Ireland, coupled with the extensive volcanics in the Antrim basalts of that region, have been taken as evidence for a proto-Icelandic plume beneath NE Ireland and western Scotland associated with the British Tertiary Igneous Province (BTIP). The most well-known artefact of the BTIP in Ireland is Giant's Causeway located on the northern coast of Northern Ireland. The BTIP is linked with the North Atlantic Tertiary igneous province that began erupting at 62 Ma (Kirstein and Timmerman, 2000). Al-Kindi et al. (2003) re-analyzed the complete dataset (for the first time) from the UK/Ireland CSSP/ICSSP (Bott et al., 1985; Jacob et al., 1985) as a single profile, and modeled the dataset together with sedimentary history and gravity data. They mapped an anomalous mantle region extending to NE Ireland that they interpreted as a hot convective sheet that initiated at ca 63 Ma. Arrowsmith et al. (2005) modeled teleseismic travel times for Ireland and UK stations, and imaged a low-velocity anomaly spatially coincident with the BTIP, providing further support for the anomaly being associated with a convective plume head that became trapped beneath thinned lithosphere at ca 60 Ma.

3. Data available

The primary data that we use for our exploration of Ireland's lithospheric thickness are (1) topography, (2) Bouguer anomalies, (3) geoid height, and (4) surface heat flow. In addition, we take information from seismology and geochemistry to constrain the crust and the range of possible chemical compositions for the lithospheric mantle.

3.1. Topography

The filtered topography of Ireland is shown in Fig. 1. The GTOPO30 data were gridded using GMT's (Generic Mapping Tools, from Wessel and Smith, 1998) routine *surface* with a 1 minute interpolation interval and with internal and boundary tensions set to 0.25 and 1.00 respectively. The grid was then long-wavelength filtering using GMT's routine *grdfilter* with a 1 minute interpolation interval and cosine arch weighting with a width of 50 km. The island of Ireland has moderate topography, with over 30% of its landmass below 10 m and average and median elevations of 62 m and 55 m respectively. The middle of Ireland is more subdued, whereas to the north and south there is greater and higher relief. The filtered topographic data along a north–south track at a longitude of 7.75°W, the white line in Fig. 1, are plotted in Fig. 7.

3.2. Bouguer anomalies

The Bouguer gravity data for Ireland are taken from the databases of DIAS and the Geological Survey of Northern Ireland (Readman et al., 1997). The filtered Bouguer gravity data for the island of Ireland are shown in Fig. 2, using the same interpolation and smoothing algorithms and parameters as for the filtered topography map, and the north–south track is plotted in Fig. 7. The gravity low associated with the Leinster Granite in SE Ireland shows up spectacularly well. Apart from that anomalous region, Bouguer gravity ranges from a minimum of around −15 mgal to a maximum of around +35 mgal, with mean and median values both of 15 mgal.

The gravity measurements were reduced for terrain to Bouguer anomaly values using a standard density of 2670 kg m^{-3}. The visible anti-correlation between the Bouguer anomaly low over the Leinster Granite in SE Ireland and the topographic high attests to the presence

of light granitic rocks that are over-compensated with that reduction density. Thus, a simple 2D model with no granitic bodies included has to result in a gentle regional increase in Bouguer gravity from south to north on the order of 10–15 mGal, once the local gravity effects of the granites have been stripped from the total signal.

3.3. Geoid height

The geoid database for Ireland is taken from EGM 2008 (Pavlis et al., 2008). The variation in the geoid over Ireland is ±1 m, with an average value of 57 m and an increase from east-to-west. As shown by Fullea et al. (2014-this issue), removing the long wavelengths of >4000 km (2°–9°) retains the effects of density anomalies shallower than ~400 km depth (Bowin, 2000a,b), and reduces the geoid height over Ireland to an average of around 1 m. The north–south variation is minimal — well less than 0.75 m (plotted in Fig. 7).

3.4. Surface heat flow (SHF)

Ireland is not well covered with SHF measurements. Most of them were conducted in the early 1970s by J.P. Wheildon (Imperial College London) and subsequently in the late 1970s/early 1980s by Andrew Brock (National University of Ireland, Galway) as part of the European Geothermal Energy Program. The 1984 report by Brock and Barton (1984, available at http://www.iretherm.ie/publications.html) remains the most authoritative compilation of SHF measurements to date for the whole of the island of Ireland. The 18 measurements are listed in Table 1 (first 18), six in Northern Ireland (repeated in the 1986 British Geological Survey report of Downing and Gray (1986)), and the remaining 12 in the Republic of Ireland. Further to that, four more SHF measurements, also listed in Table 1 (last four), were made in shallow boreholes into granite bodies in the Republic of Ireland in the late
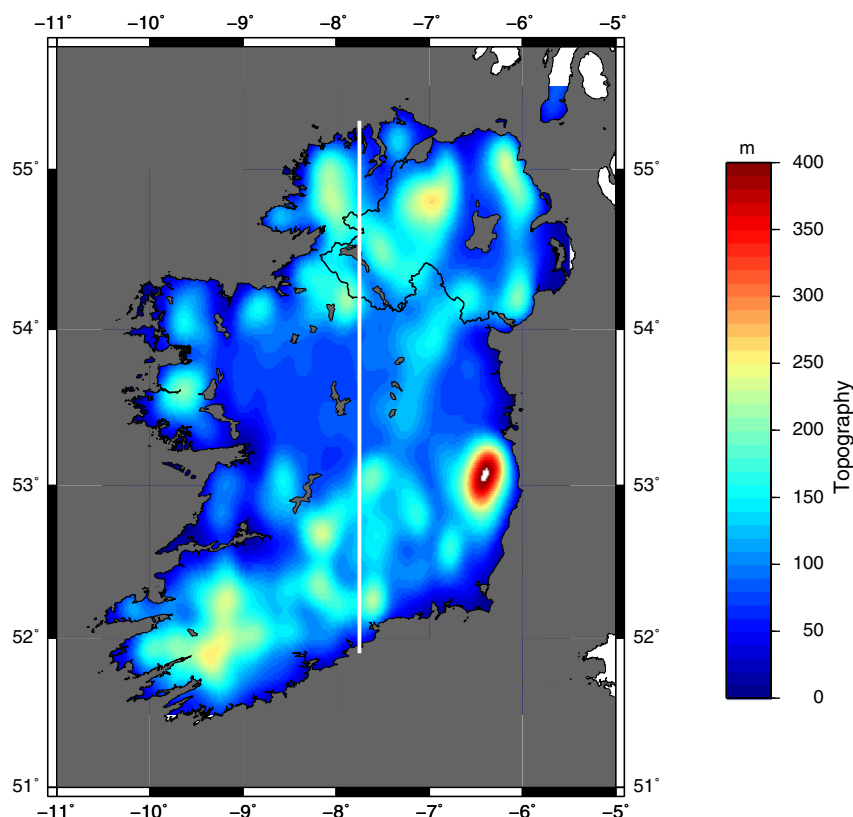

Fig. 1. Filtered topography of Ireland. Data along the north–south profile at 7.75°W are shown in Fig. 7 and are modeled to first order.
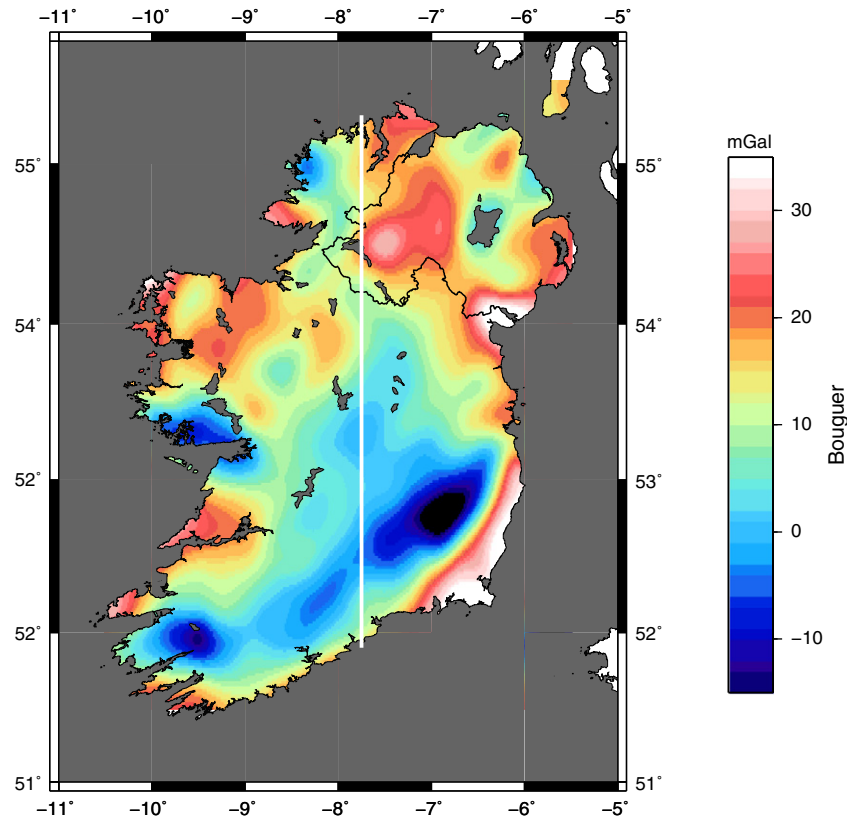
Fig. 2. Filtered Bouguer gravity of Ireland. Data along the north–south profile at 7.75°W are shown in Fig. 7 and are modeled to first order.

1980s (reported in Barton et al., 1989, also available at http://www. iretherm.ie/publications.html). Note that four of the six measurements in granites (squares in Fig. 4) have high values (Mourne Mountains,

Barnesmore, and Leinster), whereas the two in the Galway Granite have values that are consistent with regional SHF estimates in sedimentary lithologies. This suggests that at the locations where the

Table 1
Surface heat flow measurements in Ireland.

Code	Borehole	Latitude (N)	Longitude (W)	Surface heat flow (mW m^{-2})	Comment	Referenced in
D1	Portmore	55:13:43	6:19:13	81	Wheildon, uc	BB84, G86, B89, R95
M10	Killimor	53:12	8:21	66	Wheildon, uc	CR79, BB84, B89
M11	Tynagh	53:08	8:23	61	Wheildon, uc	CR79, BB84, B89
N15	Moate	53:26:50	7:40:55	70	Wheildon, uc	CR79, BB84, B89
R5	Rathkeale (also called Adare)	52:30:30	9:00:10	52	Wheildon, uc	CR79, BB84, B89
R13	Sixmilebridge	52:46	8:48	57	Wheildon, uc	CR79, BB84, B89
T1	Avoca	52:52	6:13	65	Wheildon, uc	CR79, BB84, B89
M6	Eyrecourt	53:13	8:08	60	Brock	BB84, B89
N3	Ballinalack	53:37:45	7:28:30	75	Brock	BB84, B89
N9	Navan	53:38:54	6:44:22	75	Brock	BB84, B89
N18	Castlejordan	53:24:28	7:06:57	72	Brock	BB84, B89
R2	Slieve Allaun	52:49:35	9:13:05	70	Brock	BB84, B89
R4	Courtbrown	52:38:30	8:59:30	58	Brock	BB84, B89
D2	Larne No. 2	54:50:54	5:48:33	59		DG86, B89, R95
H5	Killary Glebe	54:33:21	6:41:10	60		DG86, B89
J9	Ballymacilroy	54:47:15	6:19:50	59		DG86, B89
J10	Annalong valley	54:09:20	5:45:02	87	Wheildon, Mourne Mountains granite	DG86, B89
J11	Seefin quarry	54:08:30	5:55:03	84	Wheildon, Mourne Mountains granite	DG86, B89
	Ros a Mhil	53:15:47	9:33:11	77	Brock, Galway granite	BBS89
	Camus	53:21:36	9:35:24	65	Brock, Galway granite	BBS89
	Barnesmore	54:43:12	7:57:00	85	Brock, Barnesmore granite	BBS89
	Sally Gap	53:09:00	6:19:48	80	Brock, Leinster granite	BBS89

References: BB84: Brock and Barton (1984); B89: Brock (1989); BBS89: Barton et al. (1989); CR79: Cermak and Rybach (1979); DG86: Downing and Gray (1986); R95: Rollin (1995).
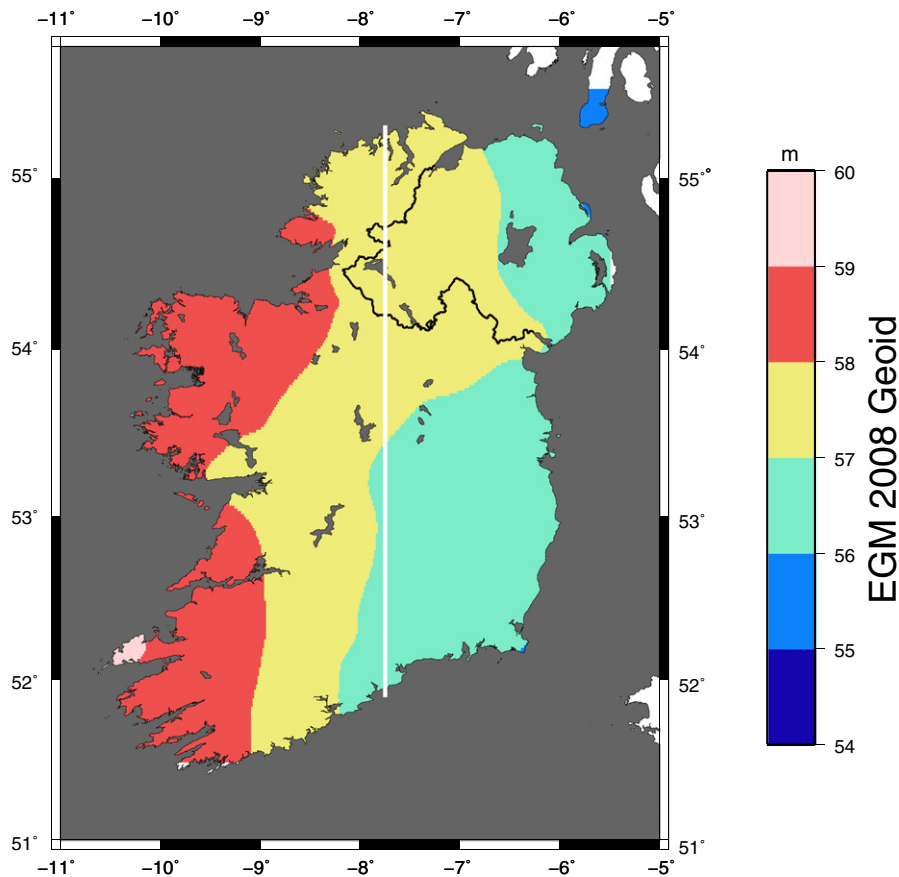
Fig. 3. EGM 2008 geoid over Ireland. Data along the north–south profile at 7.75°W are shown in Fig. 7 and are modeled to first order.

measurements were made the Galway granites are thin and their content of heat-producing elements does not add significantly to the regional SHF.

In addition to these 22 SHF measurements, there are six *estimates* of heat flow (Table 2, triangles in Fig. 4), determined by Brock and Barton (1984) from bottom-hole temperature measurements made in deep petroleum boreholes in the 1960s coupled with knowledge of the lithologies in those boreholes from well logs and average thermal conductivities assigned to those lithologies. The assumed conductivities are listed in Table 3, together with laboratory-measured values for the dominant lithologies, namely limestone, shale and sandstone. The thermal conductivity measurements made by Brock and Barton (1984) on core from boreholes are heavily dominated by measurements on limestone samples. These SHF estimates must be taken as indicative only; the large ranges of thermal conductivity for the three dominant lithologies mean that these estimates have very large uncertainties associated with them. Additionally, as well as random errors there may be bias caused by sample selection. The "typical" thermal conductivity values given in Table 3 of Brock (1979) are 3.4, 1.4 and 3.3 W m^{-1} K^{-1} for limestone, shale and sandstone respectively, which all differ from the adopted values of 3.0, 2.4 and 4.5 W m^{-1} K^{-1} (Table 3), especially for shale and sandstone. Also, we note that the average thermal conductivity of 4.5 W m^{-1} K^{-1} for sandstone derived by Brock and Barton (1984) is a factor of two greater than the 2.24 $\pm$ 0.51 W m^{-1} K^{-1} measured for the dominant Sherwood Sandstone of northern Ireland by Gunn et al. (2005). Using a smaller thermal conductivity will reduce the SHF of the anomalously high values calculated for the McNean No. 1 and Dowra No. 1 boreholes in NW Ireland (triangles in Fig. 4).

All 28 SHF values are shown in Fig. 4. Taking into account the unreliability of the six SHF estimates, and that measurements in granites will be affected by local heat production and thus will not be representative of lithospheric contributions, the SHF of Ireland is moderate and exhibits little south-to-north increase, with the sole exception of the value of 81 mW m^{-2} at Portmore on the northern coast measured by Wheildon in 1970–71. This high value was confirmed in more recent industry drilling close to Portmore (Rathlin Energy, pers. comm.). As noted below with regard to the Moho depth, the northern coast of Ireland is anomalous in both high SHF and crustal thickness.

Using the same interpolation and filtering approaches as for the topography and Bouguer gravity for the data from 15 SHF measurements in sedimentary lithologies, the low Galway granite SHF measurement plus the 3 SHF estimates from petroleum boreholes that are consistent with the nearby SHF measurements yields the new heat flow map for Ireland shown in Fig. 5. There is a suggestion in this map of a moderate increase in heat flow in the center of Ireland from 55 to 60 mW m^{-2} to some 70 mW m^{-2}, as shown in Fig. 7. However, this apparent SHF trend is tentative at this stage, as SHF measurements in Ireland are few and sparse, especially in the north.

In contrast to our analysis, Goodman et al. (2004) made a different selection of the available SHF data, and constructed a map using all available values shown in Fig. 4, both measured and estimated, with the exception of the 3 low SHF measurements made in northern Ireland labeled D2 (Larne No. 2), H5 (Killary Glebe) and J9 (Ballymacilroy) and the two granite values in northern Ireland labeled J10 (Annalong valley) and J11 (Seefin quarry). Their map can be viewed in their report (map 21B, Goodman et al., 2004), and on the website of the Sustainable Energy Authority of Ireland (www.seai.ie). (Note that on that map one of the data points is mislocated.) An SHF map constructed with this selection of values and using the interpolation and gridding parameters applied as
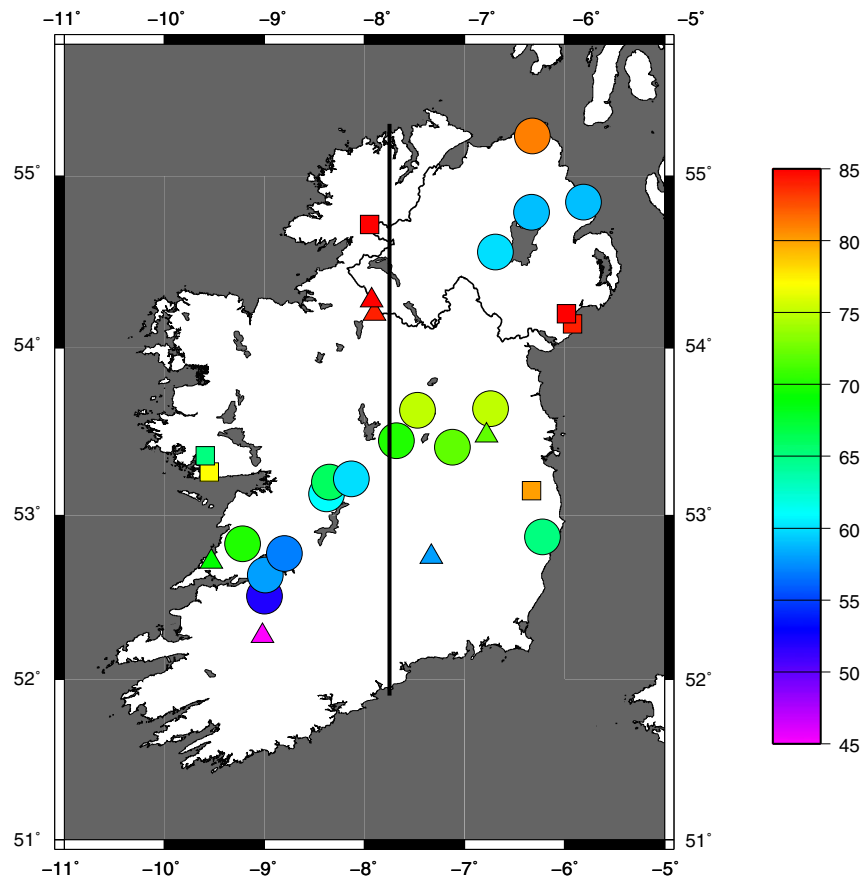
Fig. 4. Heat flow of Ireland. Circles are SHF measurements in sedimentary boreholes, squares are SHF measurements in granites, and triangles are SHF *estimates* made from bottom-hole temperature records of deep petroleum boreholes coupled with recorded lithologies and assigned thermal conductivities to those lithologies in Table 3.

above yields the map shown in Fig. 6, with the suggested strong north–south trend shown in Fig. 7. The trend has a large gradient indicative of very high heat flow in northern Ireland (>80 mW m^{-2}), low heat flow in southern Ireland (<50 mW m^{-2}), and somewhat high values in the middle (~70 mW m^{-2}). However, this trend is highly questionable, given the doubts about the estimated SHF values from the old industry bottom-hole temperatures and the neglect of the low SHF values in northern Ireland. Thus, although we do attempt to model SHF, we only model a somewhat moderate south-to-north increase.

4. Crustal information

In order to model the surface response and geophysical observables of the lithospheric mantle, it is necessary to assume physical properties and geometry information about the crust; its layering, thickness extent

(Moho) and the density and mechanical and thermal properties of each layer. In an area of scant knowledge, this can be an impediment to lithospheric modeling using LitMod. However, bounds and constraints can be derived that reflect the extent of information available.

4.1. Crustal seismology

A number of controlled-source seismological studies have been carried out in Ireland over the last three decades, and those up to the early 2000s are extensively reviewed by Landes et al. (2005). In addition, crustal receiver function studies using the ISLE teleseismic array, predominantly located in SW Ireland, were conducted by Landes et al. (2006).

The crust in the center of Ireland, at the northern end of the VARNET line, was modeled as a 7-layer isotropic 1D crust by Hauser et al. (2008), O'Reilly et al. (2010), and O'Reilly et al. (2012) (Fig. 8). Taking the stated

Table 2
Surface heat flow estimates from Marathon/Ambassador wells.

Code	Borehole	Latitude (N)	Longitude (W)	BHT depth (m)	BHT temp.	Surface heat flow estimate (mW m^{-2})	Reference
H6	McNean No. 1	54:17	7:56	1642	57.7	86	BB84
H7	Dowra No. 1	54:12	7:54	1774	63.8	84	BB84
N22	Trim No. 1	53:29	6:47	737	29.1	72	BB84
R7	Meelin No. 1	52:16	9:01	1690	33.9	40	BB84
S3	Ballyragget No. 1	52:45	7:20	1133	31.4	58	BB84
Q1	Doonbeg No. 1	52:43	9:32	957	38.9	69	BB84

BB84: Brock and Barton (1984).

Table 3
Thermal conductivities for the majority of sedimentary lithologies in Irish boreholes and assumed values in Brock and Barton (1984) for derivation of the surface heat flow estimates given in Table 2.

Lithology	No. of samples	Average ($W\ m^{-1}\ K^{-1}$)	Range ($W\ m^{-1}\ K^{-1}$)	Assumed values ($W\ m^{-1}\ K^{-1}$)
Limestone	218	3.066	1.033–5.701	3.0
Shale	3	2.423	2.206–2.826	2.4
Sandstone	4	4.645	3.442–6.160	4.5

layer velocities from those publications, the crust in southern and central Ireland has an average compressional-wave velocity (Vp) of 6.44 km/s (slowness-weighted average) to 6.46 km/s (velocity-weighted average), an average shear-wave velocity (Vs) of 3.64 km/s to 3.65 km/s, an average Vp/Vs of 1.77, an average Poisson's ratio of 0.266, and an average derived bulk density (RhoB) of 2817 kg m^{-3} (slowness weighting) to 2823 kg m^{-3} (velocity weighting) according to the updated empirical Vp-density relationship of Brocher (2005).

In regional detail, based on the velocity estimates of Hauser et al. (2008), O'Reilly et al. (2010), and O'Reilly et al. (2012) the crust in central Ireland can be characterized to first order by two layers, an upper/middle crustal layer to 23.5 km depth with a density RhoB of 2776–2778 kg m^{-3}, and a lower crustal layer from 23.5 to 31.0 km with a RhoB of 3024–3063 kg m^{-3}. We note that the latter density correlates well with the average density of five lower crustal xenoliths of 3100 kg m^{-3} measured at STP conditions (van den Berg et al., 2005).

At the southern end of the VARNET line, the average values are Vp = 6.10 km s^{-1}, Vs = 3.54 km s^{-1}, Vp/Vs = 1.71, RhoB = 2750 kg m^{-3} (from Vp), and a Poisson's ratio = 0.246. As for the northern end of the VARNET profile, these averages have been derived by arithmetically averaging the values reported in Hauser et al. (2008), O'Reilly et al. (2010), and O'Reilly et al. (2012). The anomalously low Vp is indicative of more felsic rocks. The lowermost crust (bottom 4 km) has Vp/Vs = 1.75, indicative of more mafic material, with a RhoB = 2870 kg m^{-3} and a Poisson's ratio = 0.273.

4.2. Crustal geochemistry

Information on crustal geochemistry comes from granulite-facies lower-crustal xenoliths exhumed primarily along the trace of the Iapetus Suture Zone (van den Berg et al., 2005). These xenoliths are characterized by low velocities, low density (Table 5) and high silica content compared to global averages (van den Berg et al., 2005). The average temperature-corrected Vp value for these xenoliths is 6.89 km/s, which compares excellently with the observed seismic velocity of 6.80–6.90 km/s in Layer 6 (O'Reilly et al., 2012). The density values were measured at room-temperature conditions. In order to extrapolate them to 20–30 km depth, we assume a standard crustal compressibility and thermal expansion coefficient of 1.33×10^{-11} Pa^{-1} and 2.5×10^{-5} K^{-1}, respectively (see below).

In summary, seismic velocity studies coupled with information from lower-crustal xenoliths from central Ireland suggest that the crust of Ireland is anomalously felsic, i.e., light, in comparison to typical continental crust (Hauser et al., 2008; O'Reilly et al., 2010, 2012).

4.3. Moho

Both Kelly et al. (2007) and Davis et al. (2012) compiled all of the available Moho depth estimates for the UK and Ireland, and the data
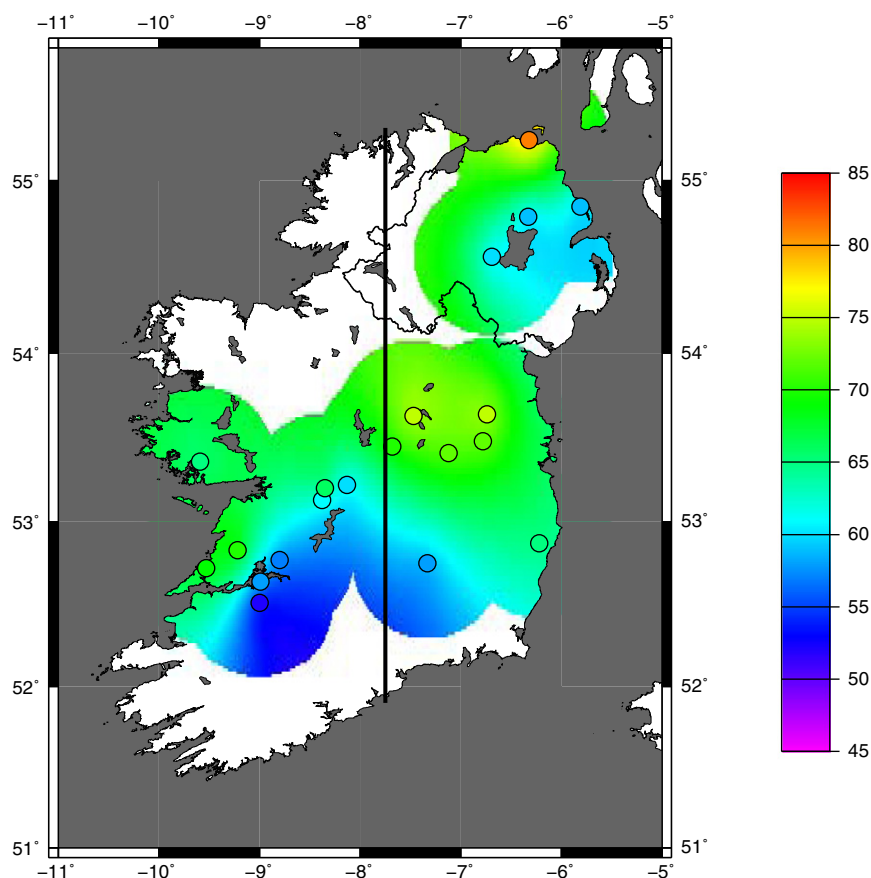
Fig. 5. Interpolated and filtered heat flow map of Ireland excluding anomalous SHF estimates and all SHF measurements in granites except for one on the Galway Granite (Camus). Data along the north–south profile at 7.75°W are shown in Fig. 7 and are modeled to first order.
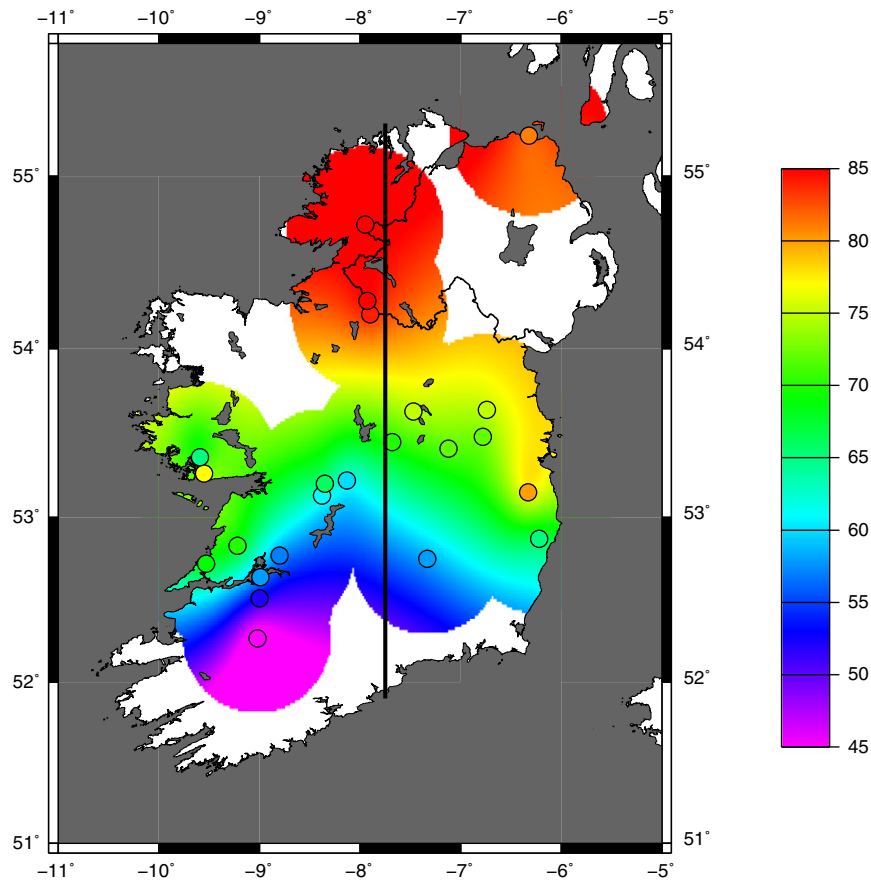
Fig. 6. Interpolated and filtered surface heat flow map using the Goodman et al. (2004) data selection.

of Davis et al. (2012) for Ireland are plotted in Fig. 9. The contour plot was constructed using the same approach and same parameters as for the previous maps (interpolation using the GMT routine *surface* and long wavelength filtering using the GMT routine *grdfilter*).

Coverage is not uniform across the island. There are far more estimates in the southern half, south of the Iapetus Suture, than in the northern half. In general, the Moho is relatively flat, with the suggestion that in the Midlands of Ireland, the Moho is somewhat shallower (28.5 km) than in the southern (31–32 km) and northern (30 km)

parts. This inference comes from the NNW-SSE profile of estimates lying close to the NS interpolation line; this is the trace of the Caledonian Onshore–Offshore Lithospheric Experiment (COOLE) Line 1, a seismic refraction survey conducted in 1985 and published by Lowe and Jacob (1989). The average crustal thickness along COOLE 1 is 30 km, with a variation of no more than ±2 km.

Mapping of the Moho by marine seismic reflection studies in the Irish Sea between Ireland and Great Britain infers a shallower Moho in the northern part (minimum 9.5 s TWTT) compared to the southern
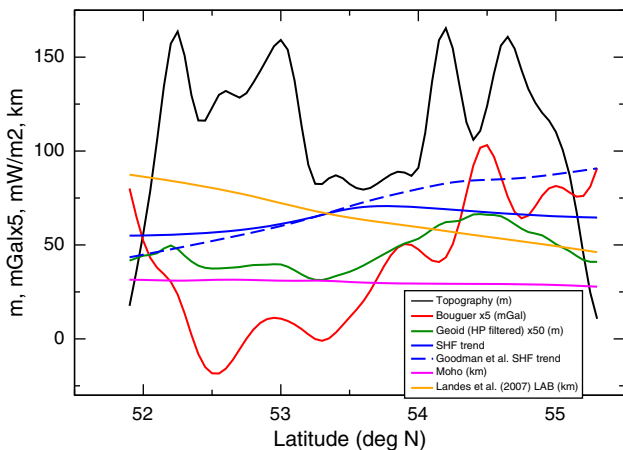

Fig. 7. North–south variation of long wavelength filtered topography, Bouguer gravity (×5), high-pass filtered geoid (×50), heat flow (both proposed new SHF map and that of Goodman et al. (2004)), Moho depth and LAB depth, along a longitude of 7.75°W.
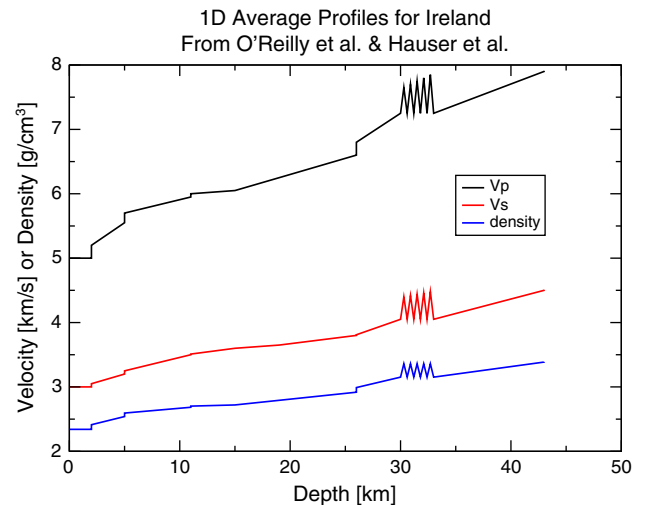

Fig. 8. 1D average velocity and density for Irish crust, from Hauser et al. (2008), O'Reilly et al. (2010), and O'Reilly et al. (2012).

Table 4
Crustal parameters.

	Thickness (km)	Density ρ (kg m^{-3})	Radiogenic heat production (W m^{-3})	Thermal conductivity λ (m^{-1} K^{-1})	Thermal expansivity α (K^{-1})	Compressibility β (Pa^{-1})
Upper crust	20	2780	10^{-6}	2.5	2.5 × 10^{-5}	1.33 × 10^{-11}
Lower crust	10[a]	3100	10^{-6}	2.5	2.5 × 10^{-5}	1.33 × 10^{-11}

[a] Lower crust is 10 km thickness in the 1D and some 2D models, but varies laterally from 9 to 11 km in some 2D models.

part (maximum 10.5 s TWTT) (Chadwick and Pharaoh, 1998). This implies a maximum of up to ca 3 km of difference for the same crustal velocity structure, and interpreted depths of 28.5 km in northern Ireland, 30 km in central Ireland, and 31.5 km in southern Ireland for a laterally and vertically uniform migration velocity of 6.0 km s^{-1}. Similarly, BIRPS seismic reflection studies in the Atlantic off western Ireland also yield crustal estimates of around 30 km.

Very recent P-to-S receiver function (pRF) estimates of Moho depths by Licciardi et al. (2013) are broadly consistent with Fig. 9, in particular with an estimate of 30 km for Ireland Array station in IAD33 located in the center of the northern part of Ireland. Licciardi et al. (2013) also find relatively thin crust for stations close to the northern coast of Ireland, consistent with previous estimates (Davis et al., 2012; Kelly et al., 2007).

In conclusion, excluding the abrupt thinning close to the northern coast, the Moho variation beneath onshore Ireland is at most 3 km, with an average value of 30 km and a suggestion of some thinning in the center of Ireland directly north of the ISZ and a south-to-north thinning trend. Minimum and maximum possible Moho depths are 28 km and 32 km respectively, whereas probable depth ranges are closer to 28.5–31.5 km. Calculations presented in Section 6.3.1 are undertaken for models with Moho depth varying within these limits to explore the relationship between Moho depth and LAB depth.

4.4. Crustal model parameters

The crustal parameters used in the modeling are listed in Table 4. The choices made, and the possible variations allowed, are examined in Section 6.3 for each parameter and ranges for topography are calculated for the ranges of each crustal parameter. Note that in these calculations, density is a function of its given STP value and calculated P,T conditions, using assumed compressibility and thermal expansivity values discussed below.

5. Mantle lithosphere information

5.1. Lithosphere–asthenosphere boundary

The lithosphere–asthenosphere boundary (LAB), the base of the plates, is a first-order feature in tectonic processes, but various geochemical and geophysical proxies for it yield different depths (Eaton et al., 2009). A statistical comparison of depth estimates in

central and northern Europe by Jones et al. (2010) showed that the seismic LAB estimated from receiver functions (sLABrf), seismic LAB estimates from seismic anisotropy (sLABa), and electrical LAB estimates from MT (eLAB) are not always in agreement. Thus, it is necessary when discussing the LAB to define precisely how it has been estimated/measured.

In this paper and the companion paper (Fullea et al., 2014-this issue), the definition of the LAB is based on temperature (tLAB) and compositional distribution (cLAB). The lithospheric mantle is defined thermally as the portion of the mantle characterized by a conductive geotherm, and compositionally as the portion of the mantle generally characterized by a different (normally, more depleted) composition with respect to the fertile composition of the sub-lithospheric (asthenospheric) mantle (i.e., PUM in Table 8). For more details of how this boundary is treated, particularly the transition zone between the conductive and adiabatic regimes, see Afonso et al. (2008), Fullea et al. (2009), and Fullea et al. (2014-this issue).

The LAB sensu stricto is given by rheological/mechanical properties, and an estimate of 71 km was recently determined for the British and Irish Isles by Bradley et al. (2011) from modeling of glacial isostatic adjustment. This rLAB estimate can be taken as an absolute minimum value, given that geophysical proxies always yield greater depths, usually by a factor of up to two on the continents (Artemieva, 2009).

Estimates of the depths to the LAB were inferred by Landes et al. (2007) from S-to-P conversions of teleseismic arrivals stacked into assigned geographic voxels of 1.7°EW by 1°NS in size, and lie in the range of 55–85 km. These sLABrf estimates, and the geographic centers of the voxels, were picked from the plots in Landes et al. (2007), and are listed in Table 6 and shown in Fig. 10, where the individual estimates are plotted as large circles on the figure together with the gridded and long-wavelength-filtered contour map. The sLABrf depths along the south–north profile are plotted in Fig. 7.

The sLABrf estimates for western Europe, as listed in the global compilation by the Potsdam group (Kind et al., 2012), list a lithospheric thickness of 90 km beneath the Dublin GEOFON station DSB. This estimate is reasonably close to the estimate of 80 km by Landes et al. (2007) for voxel 16 approximately centered on DSB (Table 6), and presumably can be taken as indicative of the uncertainty associated with the method. These shallow estimates for the sLABrf contrast with the estimates of a low velocity layer (LVL) at depths of 110–190 km from a surface wave study (sLABsw) of the path from VAL (Valentia, SW Ireland) to ESK (Eskdalemuir, central southern Scotland) by Clark and Stuart (1981). The minimum lithospheric thickness of 110 km is associated with a LVL velocity of 4.40 km s^{-1}.

In addition, thermal models of the lithosphere also suggest a greater lithospheric thickness for the thermal LAB (tLAB). For instance, defining the LAB as the depth to 1300 °C, Artemieva (2006) gives an estimate in excess of 100 km for the LAB beneath Ireland. Moreover, the thermal model of Europe from Tesauro et al. (2009) suggests depths of 130–150 km to reach the 1200 °C isotherm, assumed as the tLAB, beneath Ireland.

In summary, the majority of prior estimates of the LAB beneath Ireland suggest a depth greater than 100 km, some as large as 130–150 km. Within this context, the sLABrf receiver function estimates are anomalous, with their far shallower values of 55–85 km.

Table 5
Velocity and density information (both measured and calculated from Vp) from lower crustal xenoliths analyzed by van den Berg et al. (2005) for Layer 6, the lowermost crustal layer, in central Ireland. Vp: measured and temperature corrected compressional wave velocity (km/s); Rho: measured density (g/cm^3); RhoB: calculated density from Vp.

Sample	Layer	Vp (temperature corrected)	Rho measured	RhoB calculated
A44	6	7.48	3.23	3.11
D5	6	6.98	3.10	2.96
D14	6	7.03	2.97	2.98
D44	6	6.53	3.15	2.84
DRB6-2	6	6.45	3.07	2.82
Averages		6.89	3.10	2.94
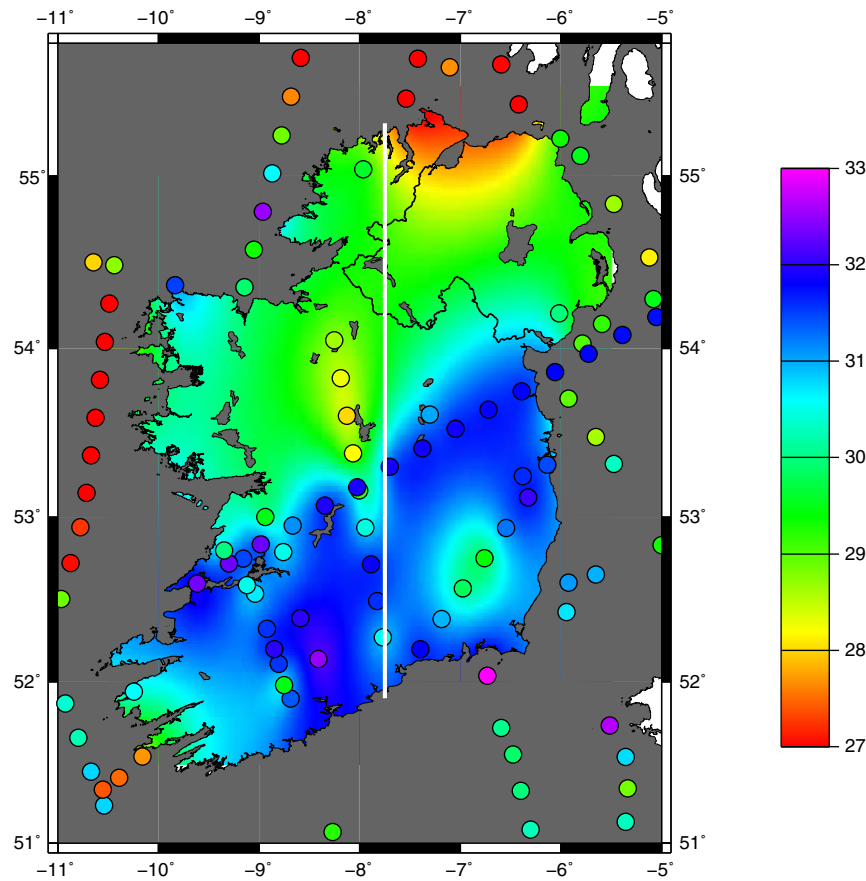
Fig. 9. Moho map of Ireland in kilometers from Davis et al. (2012). Individual Moho depth estimates shown as points, and the smoothed, interpolated, long wavelength map shown as the contoured color. Data along the north–south profile at 7.75°W are shown in Fig. 7 and are modeled to first order.

5.2. Lithospheric mantle chemistry

The only known mantle-chemistry information comes from spinel lherzolite and harzburgite xenoliths hosted in a Carboniferous alkali basalt dyke near Inver, Donegal, in NW Ireland (Gallagher and Elsdon, 1990; Shaw and Edgar, 1997). The average oxides of the six samples analyzed by Shaw and Edgar (1997) are listed in Table 7, and exhibit a somewhat depleted composition, with little CaO. Five of the six samples have a lherzolitic composition, and only one is harzburgitic, so the average is lherzolitic. This is consistent with xenoliths sampled along strike just north of the trace of the ISZ at Fidra in the Midland Valley terrane of Scotland (Downes et al., 2001). Xenolith analyses from other localities in Scotland are presented by Upton et al. (2011), who show a sharp discontinuity between pyroxenitic lower crust and a dominantly lherzolitic upper mantle. In the companion paper by Fullea et al. (2014-this issue), the Inver samples are differentiated into two sets; a lherzolitic composition (sample 3) and a harzburgitic composition (sample 6).

There are no known mantle xenoliths from the Avalon terrain in Ireland. However, along-strike xenolith samples from Darbyshire in Britain (Donaldson, 1978) exhibit an average composition that lies among global averages for spinel lherzolites.

In addition to the Inver composition, we use the bulk oxide compositions listed in Table 8 for testing our lithospheric models, taken from Afonso et al.'s averages for "Tecton" lithosphere (Afonso et al., 2008).

Table 6
Lithosphere–asthenosphere boundary depths estimated by Landes et al. (2007). Geographic locations are the centers of the voxels.

Zone	Longitude	Latitude	LAB depth (km)
1	−9.90	52.0	75
2	−10.25	52.5	70
3	−10.40	53.0	65
4	−9.00	52.2	80
5	−9.10	52.5	80
6	−9.40	53.1	75
7	−9.50	53.6	70
8	−7.95	52.2	85
9	−8.10	52.75	80
10	−8.40	53.1	70
11	−8.60	53.6	65
12	−7.00	52.9	70
13	−7.20	53.4	60
14	−7.40	53.9	60
15	−7.60	54.4	55
16	−6.00	53.3	80
17	−6.20	53.8	60
18	−6.40	54.3	60

Table 7
Oxide chemistry from Inver xenoliths (Shaw and Edgar, 1997).

	Ol (72%)	Opx (14.9%)	Cpx (2.04%)	Sp (2.32%)	Bulk
SiO_2	40.79	56.12	52.99	0.08	42.53
Al_2O_3	0.00	2.96	5.15	52.27	1.93
FeO	9.01	5.87	2.49	9.35	8.36
MgO	49.85	34.16	15.13	20.09	45.76
CaO	0.04	0.45	21.13	0.01	0.57
Na_2O	0.00	0.10	1.70	0.00	0.05

Table 8
Bulk oxide compositions.

Description	Depleted → fertile				
Oxides	Inver average	Average Tecton Peridotite	Average Spinel Peridotite	Average Tecton Garnet Peridotite	Primitive Upper Mantle
SiO_2	42.5	44.4	44.0	45.0	45.0
Al_2O_3	1.9	2.6	2.3	3.9	4.5
FeO	8.4	8.2	8.4	8.1	8.1
MgO	45.8	41.1	41.4	38.7	37.8
CaO	0.6	2.5	2.2	3.2	3.6
Na_2O	0.05	0.18	0.24	0.28	0.36
Mg#	90.7	89.9	89.8	89.5	89.3

The term "Tecton" was defined by Griffin et al. (1999) as part of the ternary Archon–Proton–Tecton classification, and refers to lithospheres for which the last tectonothermal event in the crust that was penetrated by the host volcanic rock is <1 Ga. The compositions studied by Afonso et al. (2008) range from the most depleted (Archean cratonic lithosphere) to the most fertile (Primitive Upper Mantle, PUM, of McDonough and Sun (1995)), and the Inver data lie between these two extremes, although closer to the depleted end-member. The most depleted composition (i.e., higher Mg#, depleted in Al_2O_3, FeO, and CaO, lighter) will result in the thickest possible lithosphere, whereas the most fertile (i.e., lower Mg#, heavier) will result in the thinnest possible. Thus, these two bounds of the permissible range for possible oxide compositions beneath Ireland define the maximum and minimum possible lithospheric thicknesses.

It should be noted that the range from most depleted composition we are adopting (Mg# 90.7, for the Inver lherzolite) to most fertile composition (Mg# 89.3, for PUM) represents a depletion of only 1.5 less

atoms of Fe per 100 molecules of $MgFeSiO_2$. Archean cratonic lithosphere can have far greater depletion in Fe, up to Mg# of 94, but the lithosphere beneath Ireland is not Archean in age.

5.3. Lithospheric mantle geophysical observations

Arrowsmith et al. (2005) undertook a P-wave teleseismic travel time study using data from the UK with 9 sparsely located stations on the island of Ireland. This study showed a strong P-wave low-velocity anomaly of ca. 1% at 100 km beneath NE Ireland, spatially correlated with the Paleogene BTIP magmatism, that they interpreted as a remnant of underplating by the Icelandic plume head, with no resolution for the rest of the island.

Wawerzinek et al. (2008) used data from the ISLE array (Irish Seismic Lithosphere Experiment; Do et al., 2006; Landes et al., 2007), which was located predominantly in southern and central Ireland to cover the ISZ, and imaged an anomalous north-dipping low-velocity
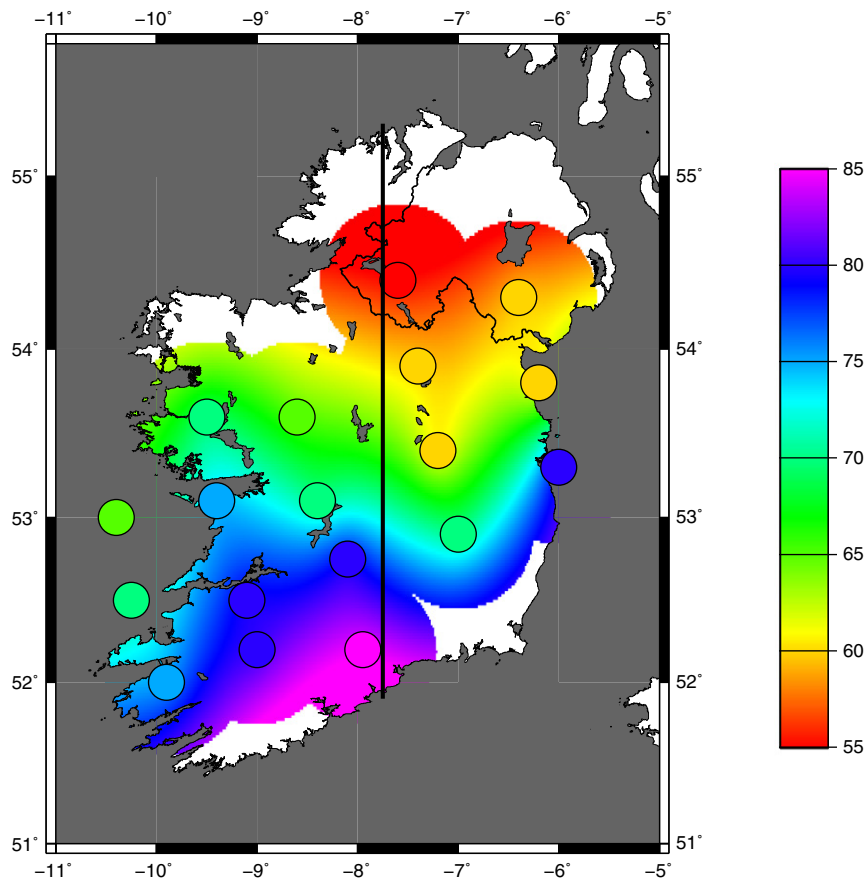
Fig. 10. LAB estimates from Landes et al. (2007). Colors are depths in kilometers.
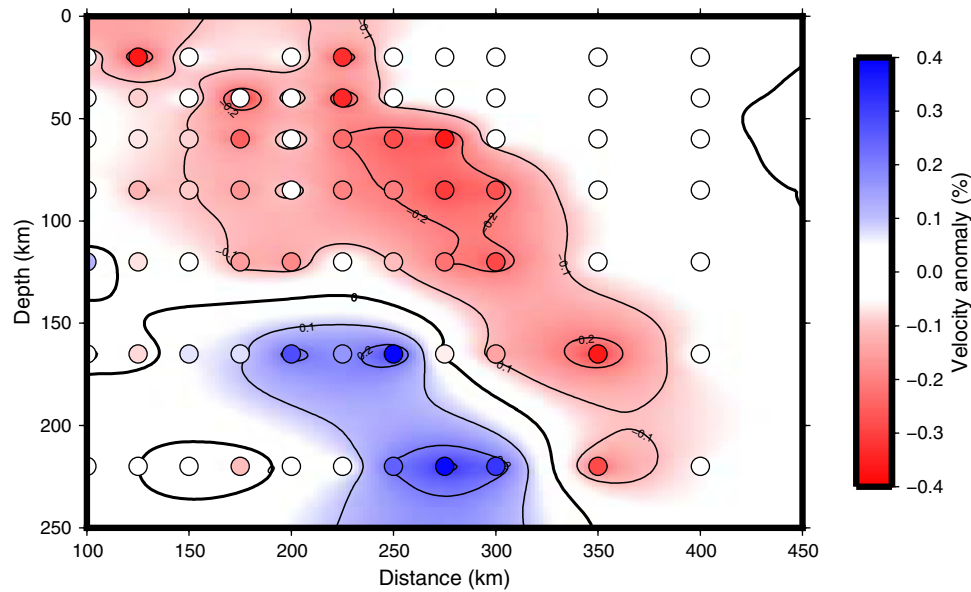
Fig. 11. N–S slice of model of O'Donnell et al. (2011) approximately along a north–south profile centered on 7.75°W. Colors are anomalous velocity values, with red being slower than average and blue being faster than average.

volume in central Ireland from P-wave travel-time tomographic modeling. They considered this anomaly to provide further support for the Icelandic mantle–plume–head hypothesis of Arrowsmith et al. (2005).

O'Donnell et al. (2011) undertook joint inversion of P-wave travel times and Bouguer gravity anomalies for the whole of Ireland using the ISLE and some of the follow-on ISUME (Irish Seismic Upper Mantle Experiment, Polat et al., 2012) stations, as well as two of the Irish National Seismic Network (INSN) stations. Coverage was far more comprehensive in southern and central Ireland and was sparse in northern Ireland (only 2 stations), with no stations north of 54.2°N. These authors identified a low-velocity anomaly in central Ireland, similar to Wawerzinek et al. (2008), but commented that "However, when interpreting the results of tomographic studies such as this, it is important to bear in mind that relative arrival time residuals remove the mean velocity structure of a region (e.g., Bastow et al., 2005; Bastow et al., 2008). In the case of Ireland, absolute P-wave delay times are fast compared to the global average (e.g., Amaru et al., 2008; Poupinet, 1979; Poupinet et al., 2003) with the implication that low velocities presented in this study are not necessarily particularly slow compared to 'normal' mantle." This general caution about misinterpretation of relative velocities in tomographic images was emphasized recently in an excellent review paper by Foulger et al. (2013).

The vertical slice through their model at the latitude of the N–S profile in the prior figures is shown in Fig. 11, where the circles are the derived velocity anomalies at the knot points in O'Donnell et al.'s (2011) 3D model; the contoured section was produced using GMT's *surface* algorithm with the internal and boundary tensions set to 0.75 and 1.00 respectively. A north-dipping low (relative) velocity structure is imaged, with a very slightly reduced P-wave velocity (~0.2%) in both lithosphere and asthenosphere that extends down to beyond 100 km.

6. 1D LitMod modeling

For details of the LitMod thermodynamic modeling framework, particularly with regard to the calculations of the stable mineral assemblages within the major oxide system NCFMAS (Na$_2$O–CaO–FeO–MgO–Al$_2$O$_3$–SiO$_2$) using minimization of Gibbs free energy (Connolly, 2005), the reader is referred to Afonso et al. (2008) and Fullea et al. (2009). The stable mineral assemblages explored in this study were

computed using Afonso and Zlotnik's (2011) modified/augmented version of Holland and Powell's (1998) thermodynamic database.

6.1. Data

The data to be modeled for Ireland in one-dimension (1D) are an average topographic elevation of 60 ± 50 m and an average surface heat flow of 60 ± 5 mW m^{-2}. Below we explore the ranges available to us for crustal and lithospheric parameters to yield a topographic elevation and an SHF acceptably close to these values. We will show how remarkably effective these two simple data are at constraining acceptable models and at falsifying unacceptable models.
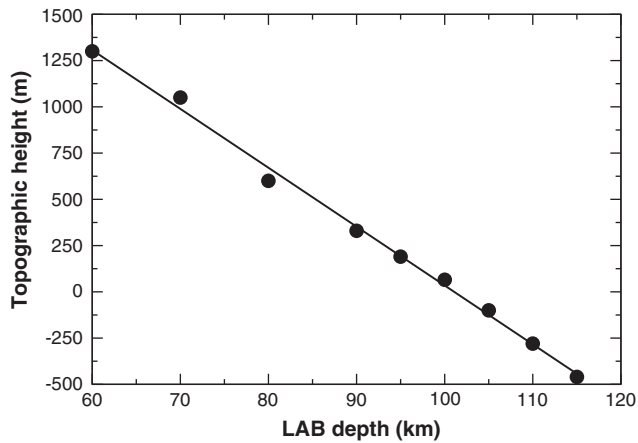
6.2. Calculations

Calculations were performed using the program LitMod2D (Afonso et al., 2008) for 1D models with the crustal values as listed above (Section 4.4) and various lithospheric thicknesses and oxide compositions. Values of topography and surface heat flow for varying lithospheric thicknesses and for the lithospheric mantle compositions given in Table 8 are listed in Table 9. For the "Average Tectonic Garnet Peridotite" this is a 2-layer lithospheric mantle with "Average Spinel

Table 9

Heat flow and absolute topography for various lithospheric thicknesses and various oxide compositions (Table 8). Areas in gray are either for significant negative topography or are unlikely. Acceptable SHF and topographic heights are indicated for given LAB depths and compositions by yellow highlighting.

Depth (km)	Heat flow	Topography (m)				
		Inver average	Average tecton peridotite	Average spinel peridotite	Average tecton garnet peridotite*	Primitive upper mantle
60	71	1350	1300	1350		1200
70	67	1050	1050	1050		950
80	64	800	600	800		500
90	61	550	330		500	160
95	60	–	190		–	0
100	59	350	65		230	
105	58		–100		100	
110	57	160	–280		–100	
115	56	60	–460			
120	56	–53				

Fig. 12. Topographic height for varying LAB depths for the "Average Tecton Peridotite" composition in the mantle lithosphere.

Table 11
Topographic height with crustal (Moho depth) and lithospheric (LAB depth) thicknesses for a crust as defined in Table 4 and oxide composition for the mantle lithosphere as defined by "Average Tecton Peridotite" in Table 8.

Lithospheric thickness	Crustal thickness		
	28 km	30 km	32 km
60 km	1000 m	1200 m	1310
80 km	630 m	800 m	970 m
100 km	−200 m	60 m	250 m
120 km	−940 m	−640 m	−330 m

that can be fit by a robust linear regression (Huber, 1981), assuming both values have error (Fasano and Vio, 1988; York, 1966, 1969), viz.
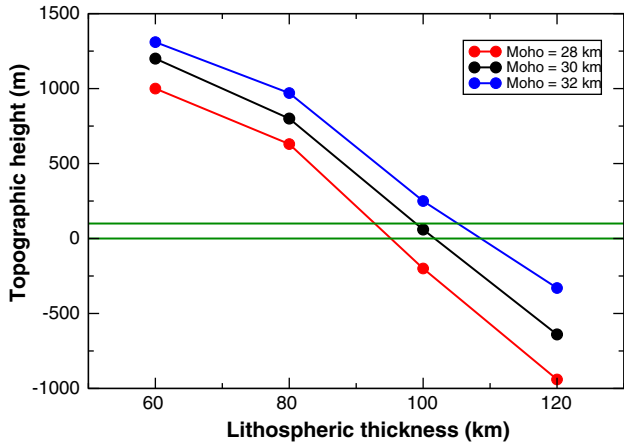
$$h_t = 3050(\pm 50) - 30(\pm 0.6) \times d_{LAB}(m) \qquad (1)$$

with a correlation coefficient of 0.999, where h_t is the topographic height (m) and d_{LAB} is the depth to the LAB (km), which must be greater than the crustal thickness (30 km). This first-order relationship is valid only for the crustal structure assumed (Table 4) and for the lithospheric composition assumed (Average Tecton Perdidotite, Table 8); it is not to be taken as generic. However, it does give us a reasonable rule-of-thumb appropriate for Ireland, and possibly also valid for Phanerozoic western Europe. It is important to note that if the thermal lithosphere was as thin as 55 km, as proposed by Landes et al. (2007) for the northern one third of Ireland (Fig. 10), then with any reasonable choice of crustal parameters and mantle compositions Ireland would be at an elevation of at least 1200 m, which is simply not observed. Even 2 km of crustal thinning, from 30 km to 28 km, would yield elevations ≥800 m.

We conclude from this analysis that the impedance discontinuity imaged in the receiver functions by Landes et al. (2007) cannot be the thermal LAB. We therefore conclude that it is a mid-lithospheric discontinuity (MLD); further discussion of this follows below.

6.3. Sensitivity to crustal parameters

Important in determining lithospheric mantle thickness from surface observations is ensuring that the crustal effects are adequately considered through appropriate choice of crustal geometry and of crustal parameters and their possible ranges. In the following we explore the possible variation in SHF and topographic height through varying the crustal parameters within likely bounds. The base model we use is that with a 30 km thick, 2-layer crust, listed in Table 4, underlain by a

Peridotite" to 80 km and very slightly more fertile "Average Tectonic Garnet Peridotite" below that.

Note that, as should be expected, when crustal parameters are not varied then surface heat flow is only a function of lithospheric thickness, and not of oxide composition. A relatively large range of LAB thicknesses, 80–115 km, will yield the observed SHF within uncertainties, as SHF is dominated by the choice of crustal parameters (see below). Far more sensitive to varying the crustal and lithospheric parameters is the derived topography. Our calculations show that the thinnest lithosphere that is consistent with the average topography in central Ireland (assuming a crustal thickness of 30 km and densities as listed in Table 4) is on the order of 90 km, and this is for dense lithospheric mantle that has been completely refertilized to the extent that it has the same oxide composition as Primitive Upper Mantle (PUM). Conversely, when we use the most depleted composition likely for the lithospheric mantle, i.e., that of the Inver xenoliths, the thickest LAB we obtain that is consistent with topography is around 115 km. A more realistic value lies between these two extremes. If we assume a reasonable lithospheric composition comprising a spinel-facies composition to 80 km and a garnet-facies composition below that, we obtain an LAB at 105 km that is consistent with the observed topography in Ireland.

A plot of topographic height against LAB depth for the "Average Tecton Perdidotite" composition shows a linear relationship (Fig. 12)

Table 10
Sensitivity of modeled SHF and topographic height outputs to varying crustal parameters. The base lithosphere is 100 km thick, with a 30 km thick crust with parameters listed in Table 4 (Moho = 30 km, density (ρ) = 2780 kg m^{-3} and 3100 kg m^{-3} in the 20-km-thick upper crust and 10-km-thick lower crust respectively, radiogenic heat production (RHP) = 1×10^{-6} W m^{-3}, thermal conductivity (λ) = 2.5 m^{-1} K^{-1}, thermal expansivity (α) = 2.5 K^{-1}, and compressibility (β) = $1.06 \times 10{-}11$ Pa^{-1}) and a mantle lithosphere defined by the oxide composition for "Average Tecton Peridotite" listed in Table 8. Model parameters are varied within likely maximum bounding limits. The approximate lithospheric thickness to get the same variation of topographic height with varying other model parameters is calculated from Eq. (1).

	Surface heat flow (mW m^{-2})	Topographic height (m)	Equivalent lithospheric thickness (km)	Effect (km)
Base lithosphere	56.6	60	98	
Moho = 28 km	55.4	−200	107	±7
Moho = 32 km	57.8	250	93	
ρ = −50 kg m^{-3} less	–	580	82	±15
ρ = +50 kg m^{-3} more	–	−680	123	
RHP = 0.74×10^{-6} W m^{-3}	50.2	−34	102	±4
RHP = 1.38×10^{-6} W m^{-3}	66.0	180	95	
λ = 2.3 m^{-1} K^{-1}	55.4	130	97	±2
λ = 2.7 m^{-1} K^{-1}	57.7	−6	101	
α = 2.25 K^{-1}	–	35	100	±1
α = 2.75 K^{-1}	–	80	98	
β = 1.06×10^{-11} Pa^{-1}	–	88	98	±1
β = 1.60×10^{-11} Pa^{-1}	–	18	100	
α = 0.0 K^{-1}, β = 0.0 Pa^{-1}	–	−8	101	+3

Fig. 13. Topographic height for varying crustal and lithospheric thicknesses for a 2-layer crust (with parameters as listed in Table 4) and oxide composition of the lithospheric mantle as given by the "Average Tecton Peridotite" (given in Table 8). The solid green lines denote topographies of 0 m and 100 m.

lithospheric mantle to 100 km with a composition defined by the "Average Tecton Peridotite" in Table 8. We vary each parameter within its likely bounds, and determine the SHF and topographic elevation. The approximate lithospheric thickness required to get the same variation of topographic elevation by varying other model parameters is calculated from Eq. (1) above for a lithospheric mantle of "Average Tecton Peridotite" composition (Table 8).

6.3.1. Moho depth
To explore the influence of changes to Moho depth, we vary the thickness of the lower crust from 8 km to 12 km, giving a variation in Moho depth from 28 km to 32 km. The introduced variation in elevation can be compensated for by modifying lithospheric thickness by ca 4 km for every kilometer of Moho variation with the same sign (see Table 10).

The topographic elevations for various Moho and LAB depths are listed in Table 11 and plotted in Fig. 13, again for a 2-layer crust (Table 4) and for the "Average Tecton Peridotite" composition in the lithospheric mantle (Table 8). The horizontal green lines in Fig. 13 denote the acceptable elevation range of 0–100 m, giving a range of permissible LAB depths of 92.5–108.5 km, i.e., 100.5 ± 8 km, for Moho depths in the range 28–32 km (30 ± 2 km).

The estimates for LABs of 80–120 km can be fit with linear regressions as follows:

$$d_{Moho} = 28\,\text{km}: h_t = 3755 - 39.25 \times d_{LAB}, \tag{2a}$$

$$d_{Moho} = 30\,\text{km}: h_t = 3675 - 36.0 \times d_{LAB}, \tag{2b}$$

$$d_{Moho} = 32\,\text{km}: h_t = 3545 - 32.5 \times d_{LAB}. \tag{2c}$$

The intercepts and gradients of these three can themselves be fit by linear regressions, to yield a formula for the topographic height as a function of both Moho and LAB depths, viz.

$$h_t = (5230 - 52.5 \times d_{Moho}) - (86.5 - 1.7 \times d_{Moho}) \times d_{LAB}, \tag{3}$$

which, for a $h_t = 0$ m, yields an expression for the LAB depth given a Moho depth,

$$d_{LAB} = (5230 - 52.5 \times d_{Moho})/(86.5 - 1.7 \times d_{Moho}), \tag{4}$$

valid for an "Average Tecton Peridotite" composition in the mantle lithosphere (Table 8). Other compositions would give similar formulae but with different constants.

Eqs. (3) and (4) can also be used for much of Phanerozoic Europe. Where the relationship between the Moho depth (d_{Moho}) and the LAB depth (d_{LAB}) is not consistent with Eq. (5), this may be taken as indicative of a different lithospheric mantle chemical composition.

6.3.2. Density (ρ)
Upper and middle crustal density (ρ) down to 20 km is assigned a uniform value of 2780 kg m^{-3}, based on an average seismic velocity for the layer of 6.27 km s^{-1} and the Vp-density empirical relations of Brocher (2005). Note that the older relationships of Christensen and Mooney (1995) yield densities of around 150 kg m^{-3} higher than the Nafe–Drake curve for velocities in excess of 6.0 km s^{-1} whereas those of Brocher (2005) fit the Nafe–Drake curve.

The lower-crustal density to 30 km is assigned a value of 3100 kg m^{-3}, based on xenoliths exhumed from 20 to 30 km depths in the center of Ireland (van den Berg et al., 2005). This density is consistent with the velocity-derived density of 3024–3063 kg m^{-3} (see above). Note that these densities are modified by temperature and pressure derivatives, according to the adopted thermal expansivity and compressibility respectively. These two factors to a large extent trade off against each other, but not completely, as discussed below.

These layer averaged density values are unlikely to be in error by more than 50 kg m^{-3}. Varying the density in the two layers by that amount for the crustal parameters as otherwise defined in Table 4 for a 100 km thick lithosphere, with a mantle composition given by the "Average Tecton Peridotite" in Table 8, leads to a large change in elevation of +520 m and −760 m for −50 kg m^{-3} and +50 kg m^{-3} respectively. (Of course there is no change in SHF.) This demonstrates the high sensitivity of topography to the assumed density of the crust in these calculations. This maximum range of elevation is equivalent to an error on the order of 15 km in lithospheric thickness (see Table 9).

6.3.3. Radiogenic heat production (RHP)
With the exception of some measurements on granites, which are superfluous to our treatment of lithospheric effects, radiogenic heat production (RHP) in Ireland's crust is poorly defined. The global compilation of Vila et al. (2010) suggests a statistical median average for the crust of $1.03 \pm (0.74–1.38) \times 10^{-6}$ W m^{-3}. We adopt a uniform value of 1.00×10^{-6} W m^{-3} for both crustal layers.

To explore the effects of varying crustal RHP, we modify our standard lithospheric model for those at the 25 percentile and 75 percentile bounds of 0.74×10^{-6} W m^{-3} and 1.38×10^{-6} W m^{-3}. Change within these extreme bounds would lead to a relatively minor SHF change of −6/+9 W m^{-2} and an elevation change of −90/+120 m (Table 10). The error probably lies within half of those bounds, thus equivalent to around ± 4 W m^{-2} for SHF and ± 50 m for topography, which translates to a variation of far less than 10 km in lithospheric thickness (see Table 9).

6.3.4. Thermal conductivity (λ)
The thermal conductivity (λ) of crustal rocks lies typically in the range 2.0–3.0 W m^{-1} K^{-1} (e.g., Kukkonen et al., 1999; Seipold, 1992), with values decreasing with depth from around 3.0 W m^{-1} K^{-1} in the upper 10 km to 2.75 W m^{-1} K^{-1} in the middle 10 km to 2.50 W m^{-1} K^{-1} in the lower 10 km (Kukkonen et al., 1999). There may be a pressure effect of up to 20% based on the work on granites by Seipold (1992), and a temperature effect of up to about 10% based on studies of amphibolites (Seipold, 1995) and up to 20% based on studies of magmatic and metamorphic rocks (Vosteen and Schellschmidt, 2003). Both of these effects will reduce thermal conductivity, and partially account for the depth variation reported by Kukkonen et al. (1999). For our calculations, λ is assumed not to have any pressure (depth) or temperature dependence, and takes an average uniform value of 2.5 W m^{-1} K^{-1} varying within possible ranges.

Modifying the thermal conductivity within the maximum possible range of 2.0–3.0 W m^{-1} K^{-1} for the crustal parameters as otherwise defined below, and for a 100 km thick lithosphere with a mantle composition given by the "Average Tecton Peridotite" in Table 8, leads to a small SHF change of −3.2/+2.5 W m^{-2}, but a relatively large change in topography of −190 and +200 m for λ = 3.0 W m^{-1} K^{-1} and λ = 2.0 W m^{-1} K^{-1}, respectively. This is because, keeping all the other parameters fixed, increasing the thermal conductivity in the crust tends to "cool down" a lithospheric column in steady state. More likely variations in the range 2.3–2.7 W m^{-1} K^{-1}, i.e. an error of up to ± 0.2 W m^{-1} K^{-1}, lead to an SHF error of ± 1 W m^{-2}, and a topographic error of ca ± 70 m (Table 10). These values are equivalent to an error of about 5 km in lithospheric thickness (see Table 9).

6.3.5. Thermal expansivity (α)

The adopted coefficient of thermal expansion (or thermal expansivity) α is assumed to be constant for both crustal layers and equal to 2.5 × 10^{-5} K^{-1}. The layer average value of α is unlikely to be incorrect by more than ± 10%, so we test the effects of thermal expansivity values between 2.25 × 10^{-5} K^{-1} and 2.75 × 10^{-5} K^{-1}. Varying α between these limits results in a very minor change of ± 25 m in elevation, which can be compensated by a ± 1 km change in the depth to the LAB. These ranges are well within the error levels of the calculations.

6.3.6. Compressibility (β)

The adopted pressure dependence of density (compressibility) β is a linear, uniform, isotropic value of 1.33 × 10^{-11} Pa^{-1} for both crustal layers. Measurements by Brace (1965) on a variety of rocks showed that at pressures greater than 1 kbar a linear dependence with pressure is valid. Crustal rocks can show a range of compressibilities, from ~1.01 × 10^{-11} Pa^{-1} for augite to ~2.68 × 10^{-11} Pa^{-1} for quartz, with dolomite being 1.21 × 10^{-11} Pa^{-1} (Brace, 1965). We thus vary compressibility within 20%, i.e. 1.06 × 10^{-11} Pa^{-1} to 1.60 × 10^{-11} Pa^{-1}, to test the sensitivity to the choice of this parameter.

Varying β between these limits has a minor effect of ± 30–40 m on elevation, which can be compensated by a ± 1 km change in the depth to the LAB. Again, these ranges are well within the uncertainties of the calculations. Calculations that exclude the effects of thermal expansivity (α set to 0.0 K^{-1}) and compressibility (β set to 0.0 Pa^{-1}) on density in the crust result in a topography that is approximately 70 m lower than that calculated when including them (Table 10). This is equivalent to an uncertainty on the order of 3–4 km in the depth to the LAB.

7. 2D LitMod modeling

We wish to determine the permissible south-to-north thickness variation in the LAB for plausible variations in lithospheric composition and Moho depths. We begin with simple geometries, and include complexity as needed to satisfy the observations. We examine end-member cases, namely the most depleted likely lithospheric mantle in southern Ireland, given by the Inver lherzolite xenoliths (Gallagher and Elsdon, 1990; Shaw and Edgar, 1997), and the most fertile lithospheric mantle in northern Ireland, given by Primitive Upper Mantle of McDonough and Sun (1995). The latter is motivated by the suggestion of modification of the lithospheric mantle of northern Ireland by a hot upwelling associated with the Icelandic plume head during initiation of the BTIP (Arrowsmith et al., 2005).

We assume that the contact between the two lithospheric layers is a simple boundary, initially vertical but subsequently with a northwards slope to explain the more subdued topography of central Ireland and to be consistent with the seismic topographic images of O'Donnell et al. (2011). We initially model the crust as flat, but subsequently we allow a slightly deeper Moho in the South (31–32 km) compared to the north (29–30 km) on either side of the Iapetus Suture, as depicted in Figs. 7 and 9 from the Moho depth compilation of Davis et al. (2012).

For simplicity, we do not consider the ocean to the north or south, but assume that the land extends to ± infinity. In the model domain, the center of Ireland is at a position of + 300 km.

7.1. Data

The data that we have to explain in our modeling are the surface heat flow (Fig. 5), the topography (Fig. 2), the geoid (Fig. 3) and the Bouguer gravity (Fig. 2). Their variations along a north–south profile at longitude 7.75°W are shown in Fig. 7.

We wish to mimic a surface heat flow that is somewhat colder to the south (60 mW m^{-2}) compared to north (70 mW m^{-2}) (Fig. 7). This is a poorly defined variation; as the SHF map (Fig. 5), excluding dubious points and SHF values from granites suggests that with the exception of the high SHF observed on the northern coast (Portmore borehole), the SHF in northern Ireland decreases back to lower values than in the center of Ireland.

Topography is subdued in central Ireland (average of + 50 m), and is higher in the southern and northern thirds of the island (averages of + 100 m) (Fig. 7). We mimic this second-order effect in our two final two-dimensional (2D) models, which includes a dipping lithospheric geometry.

The geoid increases by ca 0.75 m from southern to northern Ireland (Figs. 3, 7).

Bouguer gravity (Figs. 2, 7) shows a south-to-north increase of 20 mgal from −5 mgal to + 15 mgal (Fig. 7). Some of this increase (up to 50%) is due to low-density granitic bodies not accounted for in this paper. More details on the gravity effects of granitic bodies in Ireland are given in the companion paper by Fullea et al. (2014-this issue).
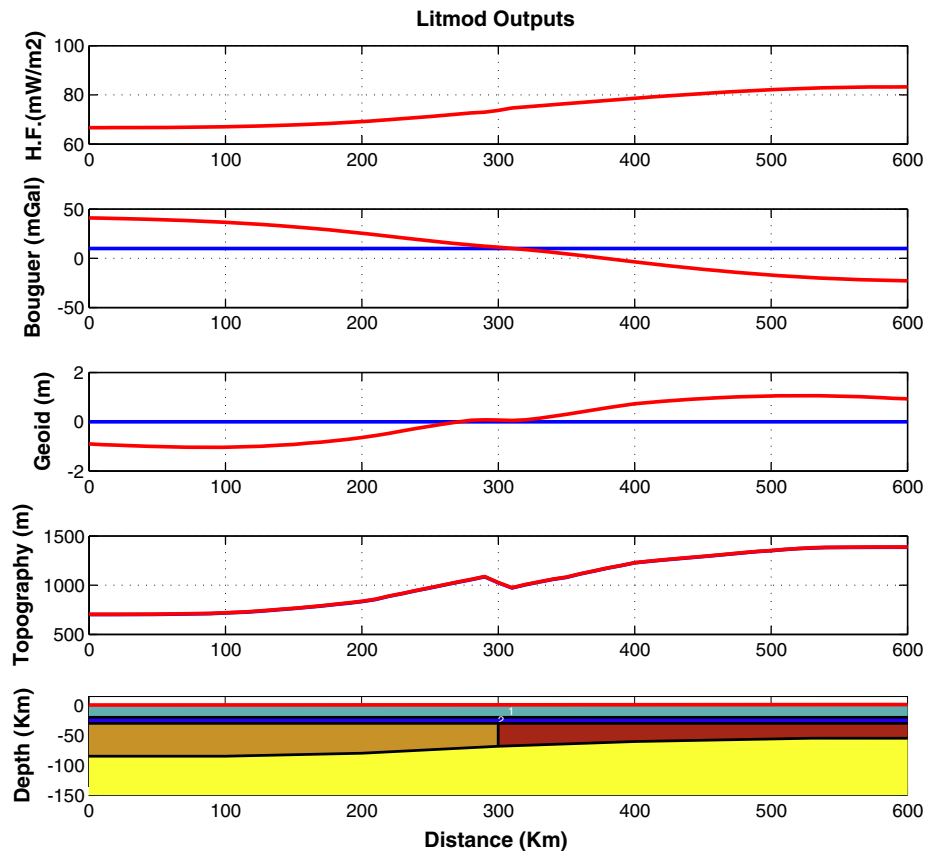
7.2. Calculations

As in the 1D models above, calculations were performed using the LitMod approach of Afonso et al. (2008). For the first three models, only approximate data are used to derive the first order effects. For the fourth model, which attempts to replicate most of the data features, the real observations are considered.

7.2.1. Landes et al. model

As the first 2D model, we test the lithospheric-thickness variation proposed by Landes et al. (2007) from sLABrf estimates; this variation is from 85 km in the south to 55 km in the north, with the 30 km of thinning occurring over <150 km. We assume a fertile mantle to the north, namely the PUM composition listed in Table 8, and a depleted mantle to the south, the Inver composition in Table 8. Such a choice for the oxide chemistry of the two lithospheres will lead to the largest allowable differences in lithospheric thickness for a given crustal structure. This is motivated by the suggestion of Landes et al. (2007), based on the prior studies of Al-Kindi et al. (2003) and Arrowsmith et al. (2005) showing that the British Tertiary Igneous Province extended into NE Ireland (Giant's Causeway), that the lithosphere beneath northern Ireland has been modified and partially removed and/or enriched. For simplicity, in this initial 2D model the crust is assumed to be laterally uniform with a thickness of 30 km.

The surface parameters that would be observed for such a model lithosphere are shown in Fig. 14. There would be a significant topographic increase of over 700 m, from an elevation of 700 m in the south to 1400 km in the north, together with a change in Bouguer gravity of over 80 mGal and a geoid variation of over 2 m, plus an increase in surface heat flow by 15 mW m^{-2}, from 67 mW m^{-2} to 83 mW m^{-2}. None of these are observed, particularly the high topography. Varying any or all of the crustal parameters within their possible ranges will not compensate for these modeled observations. Also, choosing any other mantle compositions between the two end-members will amplify the calculated N–S variations. On this basis, we can exclude the

Fig. 14. LitMod2D calculations for the Landes et al. (2007) lithospheric model with 30 km of thinning from 85 km to the south to 55 km to the north, and depleted mantle (Inver oxide composition, Table 8) to the south and fertile mantle (PUM oxide composition, Table 8) to the north. A flat Moho at 30 km with a vertical discontinuity between the two lithospheric domains is assumed. Top panel: South-to-north surface heat flow variation (red line): Second panel: Bouguer gravity variation (red line, blue line is flat Bouguer response); Third panel: Geoid variation (red line, blue line is zero geoid); Fourth panel: Topographic variation (red line); Bottom panel: Lithospheric model.

suggestion by Landes et al. (2007) that the LAB varies from 85 km in southern Ireland to 55 km in northern Ireland.

7.2.2. 112 km to the south and 94 km to the north

For the second test we use the lithospheric thicknesses given by the 1D modeling for the two mantle compositions (Table 9), of 112 km in southern Ireland for the depleted Inver composition and 92 km in northern Ireland for the fertile PUM composition. Again, a flat Moho is assumed without any lateral variation in crustal parameters.

The surface responses that would be observed are shown in Fig. 15. Ignoring the discontinuity at distance x = 300 km, which is due to the sharp vertical discontinuity imposed on the mantle compositions, the topography is essentially flat and close to the uniform value of +100 m. Bouguer gravity is also essentially flat, as is observed (to first order), as is the geoid, except in the vicinity of the discontinuity. Heat flow increases from 59 mW m^{-2} to the south to 64 mW m^{-2} to the north, a small variation of some 5 mW m^{-2}. This model thus describes the observations to first order.

7.2.3. Transitional wedge

The discontinuous topography in the above model (Fig. 15) can be made continuous and flatter by assuming a transition between the two mantle regions, modeled here as a wedge with a northwards dip in order to replicate the feature seen in the topographic image of O'Donnell et al. (2011) and shown in Fig. 11. The wedge, with fertile (PUM) mantle to the north comprising the hanging wall, also explains the somewhat subdued topography in the center of Ireland. For these calculations, the crust is also varied from 31 km in the south to 29 km in the north over a distance of 150 km (x-locations 250 to 400),

consistent with the Moho map in Fig. 9. Otherwise, crustal parameters are laterally invariant.

The surface responses that would be observed are shown in Fig. 16, and the topography is mimicked reasonably well with an average of 50 m in the center of Ireland and 100 m to the south and north. As before, heat flow increases from 58 mW m^{-2} in the south to 64 mW m^{-2} in the north, a small variation of some 6 mW m^{-2}. The variation in geoid height is around ±0.4 m, close to what is observed. Bouguer gravity shows an increase of some 20 mGal, which is indeed what is observed (Figs. 2, 7). A southwards-dipping wedge would result in increased topography in the center of Ireland, rather than reduced topography, and thus is excluded based on the actual topography.

Thinning the northern lithosphere even more to 85 km, i.e., a total of 30 km of thinning as suggested by Landes et al. (2007), yields a topographic differential of over 200 m, which is not observed (Fig. 16). Thus, for the extreme compositional variation and the assumed crustal structure, a change of the LAB depth from south to north over 150 km of some 20 km can be accommodated, but greater changes would require modifications to the lithospheric model that are difficult to justify in light of the available data (see also Fullea et al., 2014-this issue).

7.2.4. Refertilized lower lithospheric mantle to the north

A far more plausible and realistic lithosphere model, compared to the end-member models discussed above, is a Spinel Peridotite upper lithospheric mantle layer and a garnet peridotite lower lithospheric layer; assuming that refertilization by the putative Icelandic plume only affected the uneroded lower lithosphere in northern Ireland, leaving the upper lithosphere primarily unaffected. We model this with three lithospheric layers, rather than two as in the prior models. We also model a more realistic crust based on the seismic observations reported above.
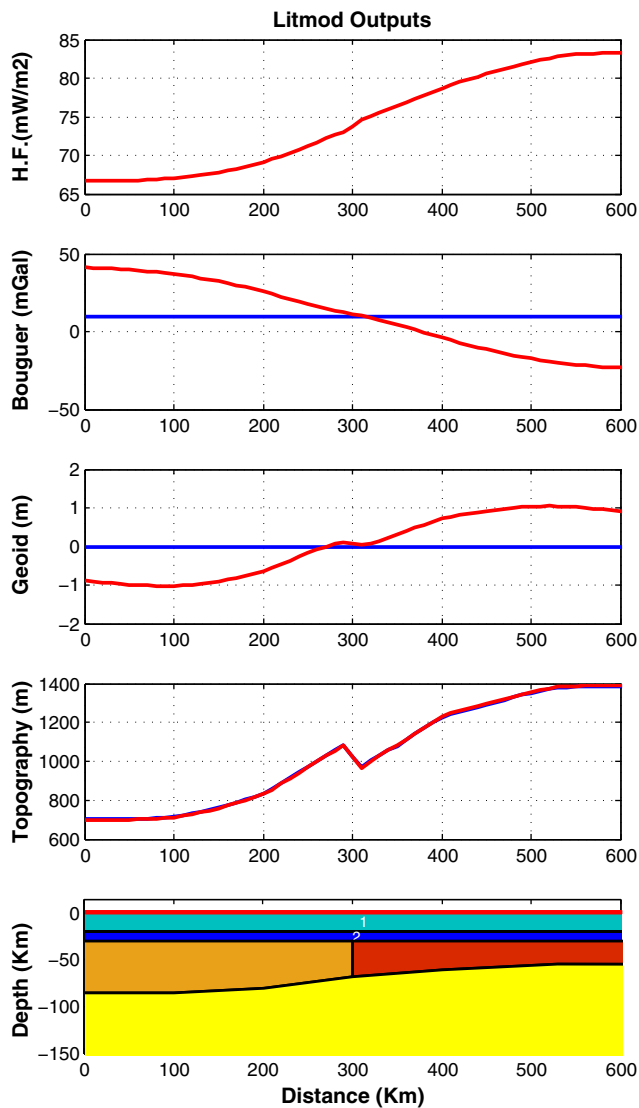
Fig. 15. LitMod2D calculations for a lithospheric model with 22 km of thinning from 112 km to the south to 92 km to the north, and depleted mantle (Inver oxide composition, Table 8) to the south and fertile mantle (PUM oxide composition, Table 8) to the north. A flat Moho at 30 km with a vertical discontinuity between the two lithospheric domains is assumed. Panels same as for Fig. 14.

The upper crust to 20 km is assumed to be laterally and vertically uniform in physical parameters, but the lower crust below 20 km is divided into two distinct layers in either side of the ISZ with a density of 3100 kg m^{-3} to the north of the ISZ, and a density of 3050 kg m^{-3} to the south of it. This is consistent with the lateral variation in velocity reviewed above (Section 4.1). Moho is varied in depth to replicate the results from the COOLE profile of Lowe and Jacob (1989), with a deeper Moho south of the ISZ (32 km), crustal thinning directly north of the ISZ to 29.5 km, then moderate thickening to 30 km beyond that.

The upper lithospheric mantle layer of "Average Spinel Peridotite" we model with a depth to 85 km to the south, and to 55 km to the north (Table 8). The depths to the bottom of this composition are chosen based on the sRF results of Landes et al. (2007), who observed strong S-to-P conversions at an upper mantle boundary that they interpreted (erroneously) as the LAB.

The lower lithospheric mantle to the south comprises a layer from 85 km to 104 km depth with the composition of "Average Garnet Peridotite" (Table 8). To the north, we assume a refertilized composition of Primitive Upper Mantle for the lower lithospheric mantle layer to

96 km, as suggested by the 1D calculations in Table 9. The geometry of the LAB reflects that of the Transitional Wedge, discussed above.

Given the arguments presented above, the boundary between the upper and lower lithospheric layers cannot be the thermal/seismic LAB, but must be a mid-lithospheric discontinuity (MLD), which we assume here is coincident with a compositional variation. Note that we do not imply that the S-to-P conversions observed by Landes et al. (2005) are the result of a compositional change alone. There may be other factors contributing to the strong conversions at this depth, such as textural changes and anisotropy changes. We only assume that this discontinuity coincides with a significant change in the average composition of the lithospheric mantle.

The surface responses that would be observed for this model are shown in Fig. 17, and the geotherms for southern, central, and northern Ireland in Fig. 18. Topography is mimicked well, with relief higher to the north and south and more subdued in the center. Heat flow increases from 59 mW m^{-2} in the south to 63 mW m^{-2} in the north, a minor variation. The geoid is almost perfectly replicated, with a 1 m increase from south to north. The Bouguer anomaly has the correct positive trend with increasing latitude, but is only around 10 mGal whereas the observations show a change of 20 mGal. However, as discussed in the section on Bouguer anomalies above, the regional Bouguer anomaly shows a north–south increase of about 10–15 mGal after the gravity effects of large granitic bodies (not accounted for in this paper) have been removed.

For this model, there is a significant horizontal temperature gradient within the lithospheric mantle. At 75 km depth, southern Ireland is at 965 °C, central Ireland is at 1050 °C, and northern Ireland is at 1100 °C. Thus a gradient of ~1 °C per kilometer occurs in the transition region. When we adopt this geometry that juxtaposes depleted lower lithosphere to the south with fertile lower lithosphere to the north, then no more than ~20 km variation in the depth of the LAB is permitted over 150 km between the south and the north. Greater variations of LAB depth lead to N–S topographic variation, as well as variations in geoid height and Bouguer anomaly, that are inconsistent with observations.

8. Discussion and conclusions

The chemical and physical structures of the lithospheric mantle affect many observables on the Earth's surface, with surface heat flow, geoid, and gravity anomalies being the obvious ones that are sometimes modeled, but also it significantly affects topography, which is rarely modeled. It is incumbent upon us to ensure that the models of the lithosphere derived from our data respect as many of these observables as possible. One cannot and should not willfully ignore or disregard data, and make interpretations that are bereft of self-consistency.

In this paper we have shown, through first-order considerations, that the thermal LAB (tLAB) beneath Ireland lies in the range 90–115 km for a crust of 29–32 km with the crustal parameters listed in Table 4. Errors introduced due to incorrect crustal parameterization will lead to a maximum variation in the LAB depth of the order of ± 15 km; crustal density has the greatest effects and Moho depth the next largest (Table 10). Thus, a lithosphere as thin as 75 km in northern Ireland at 54.5°N is permissible with an appropriate combination of crustal parameters and assumptions about lithospheric mantle composition. Even so, this would require that all of the lithosphere from the Moho down has the composition of PUM. In a more reasonable scenario the lithosphere below 55 km has been refertilized (PUM), in which case the minimum lithospheric thickness is 80 km, and more likely 95 km. Lithosphere that is as thin as the value of 55 km of Landes et al. (2007) is impossible to reconcile with surface observations under any reasonable choice of parameters; it is quite simply impossible. Even less permissible is a rapid change of 30 km over less than 150 km in north–south extent, as that would require significant
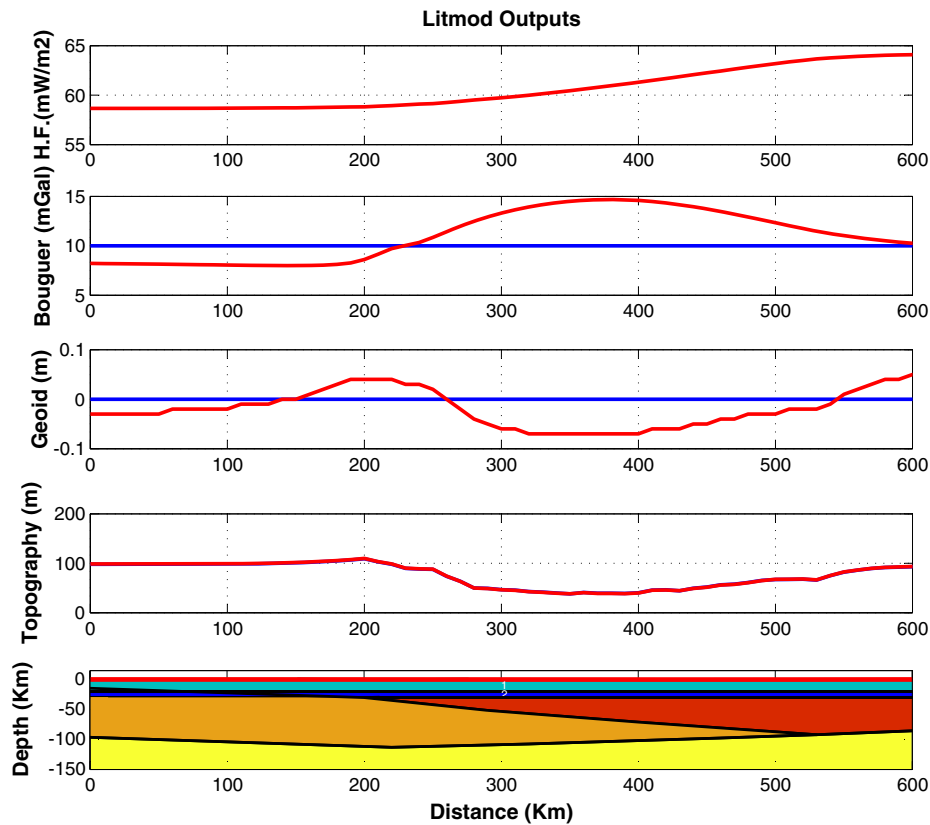
Fig. 16. LitMod2D calculations for a lithospheric transitional wedge lithosphere with 22 km of thinning from 112 km to the south to 90 km to the north, and depleted mantle (Inver oxide composition, Table 8) to the south and fertile mantle (PUM oxide composition, Table 8) to the north. In addition, the Moho thins from 31 km to the south to 29 km to the north. Panels the same as for Fig. 14.

changes in crustal parameters and crustal thickness that are not compatible with the lateral variations in Bouguer anomaly or the geoid height. A change of up to 20 km is possible, but not more. This is explored further within a 3D framework in the companion paper by Fullea et al. (2014-this issue).

Landes et al. (2007) undoubtedly imaged a relatively strong impedance interface in their S-to-P receiver functions that shallows from 85 km in the south to 55 km in the north beneath Ireland, but to label it as the LAB was erroneous and is at odds with not only petrological arguments presented here but also the northward dip of the lithospheric trace of the ISZ. What that interface is remains to be conclusively determined. Here, for our modeling we have assumed that it coincides with a compositional change in the lithospheric mantle. We do not imply that this compositional change is the ultimate reason for the observed S–P conversions, only that if a relatively sharp change in composition exists (which explains other geophysical data as well), the interface may as well be the locus of other heterogeneities (textural, anisotropy, frozen melt, etc.). If this seismic discontinuity is associated with a phase change from spinel to garnet that occurs in the region of 50–90 km (e.g., Robinson and Wood, 1998; Su et al., 2010), this would provide a significant density change (about 3%) and a high impedance contrast, but the gradient is in the wrong direction. However, mid-lithospheric discontinuities are becoming more frequently observed (e.g., Ayarza et al., 2010). Candidates to explain an S-to-P conversion at a mid-lithospheric discontinuity (MLD) are discussed by Abt et al. (2010).

This is another example of the care that we must take when we label geophysical interfaces. Even the Moho, ubiquitously used as defining the crust–mantle boundary, is sometimes not the same as the petrologically-defined crust–mantle boundary (e.g., Giese et al., 1999; Janik et al., 2009). In particular, defining the depth to the LAB is fraught

with difficulty, given not only the different proxies (e.g., Eaton et al., 2009; Jones et al., 2010) but also that the very nature of the LAB depends on whether one is mapping a mechanical, thermal or chemical boundary layer (Artemieva, 2009). In their global receiver-function study, Rychert and Shearer (2009) mapped an S-to-P converted phase that spatially correlates with tectonics, varying from 95 ± 4 km beneath Precambrian shields and platforms to 81 ± 2 km beneath tectonically altered regions and 70 ± 4 km at oceanic-island stations. While the imaged interface beneath tectonically altered regions and oceanic regions may be the LAB, it clearly cannot be the case for Precambrian shields and platforms where the LAB lies some 100+ km deeper.

Our final model not only is consistent to first order with most prior observations, but also has plausible mantle chemistry. It is however rather exotic in having a highly fertile lower lithosphere beneath northern Ireland. It is certainly not the only model that fits all of the disparate data, but it does contain the elements of features that must be in any of the acceptable models. The one observation that is not replicated is that of an albeit weak (0.25% negative velocity anomaly) north-dipping structure in the topographic slice of O'Donnell et al. (2011) from just below the Moho to 200+ km depth. We have a north-dipping lower lithosphere, but a south-dipping upper lithosphere. Also, we do not have any lateral variation within the asthenospheric layer. However, we note the caveats expressed recently by Foulger et al. (2013) regarding (over) interpretation of seismic tomographic images, especially effects such as "depth leakage", or downward smearing, and the caveats regarding images of relative velocities compared to absolute velocities.

The only solution to these apparent dichotomies is to undertake integrated modeling within an internally self-consistent petrological–geophysical framework. The LitMod approach (Afonso et al., 2008; Fullea et al., 2009, 2011) offers such a framework, and can be used in a hypothesis-testing approach, as in this paper, or a full forward-
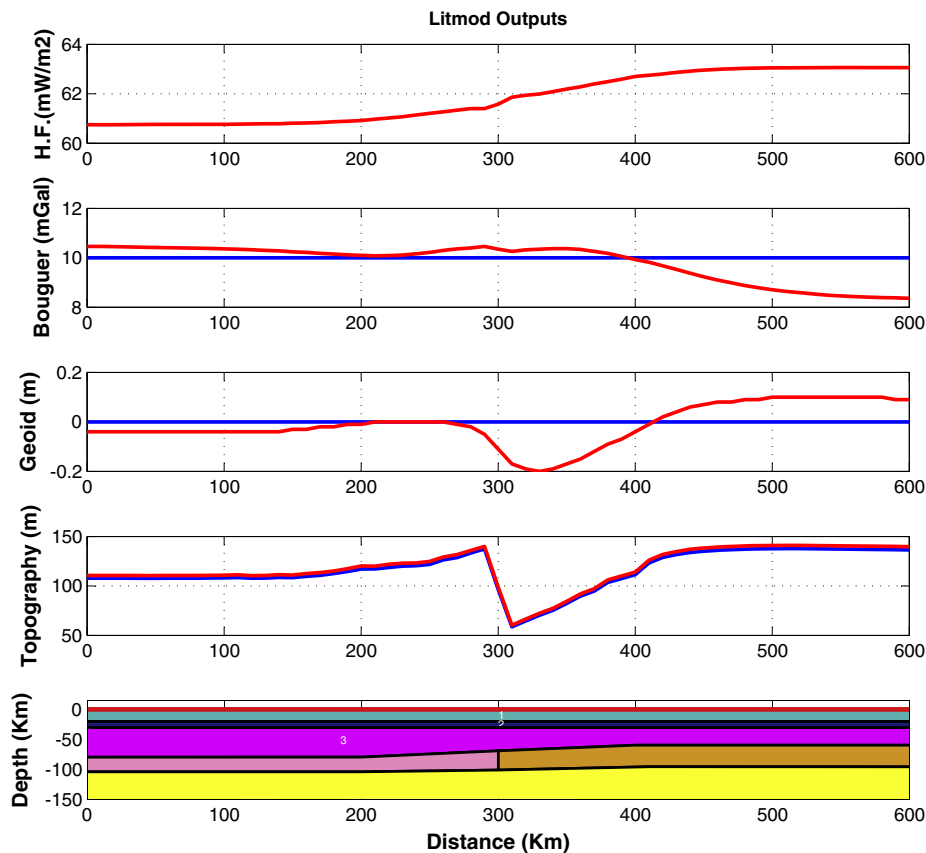
Fig. 17. LitMod2D calculations for a model that has a uniform upper crust to 20 km, and lateral lower crustal variation in depth and density. Underlying the crust is a Spinel Peridotite composition upper lithospheric mantle later to 85 km in the south and 55 km in the north. The lower lithosphere has a transitional wedge with 8 km of thinning from 104 km to the south to 96 km to the north, and depleted mantle (Inver oxide composition, Table 8) to the south and fertile mantle (PUM oxide composition, Table 8) to the north. Panels the same as for Fig. 14.

modeling approach, as in the companion paper by Fullea et al. (2014-this issue), or indeed in a full inversion approach (Afonso et al., 2013a, 2013b).

Fig. 18. Geotherms for southern Ireland (black), central Ireland (red) and northern Ireland (blue) based on the model shown in Fig. 17.

References

Abt, D.L., Fischer, K.M., French, S.W., Ford, H.A., Yuan, H., Romanowicz, B., 2010. North American lithospheric discontinuity structure imaged by Ps and Sp receiver functions. Journal of Geophysical Research—Solid Earth 115.

Afonso, J.C., Zlotnik, S., 2011. The subductability of continental lithosphere: the before and after story, arc–continent collision. Frontiers in Earth Sciences 53–86.

Afonso, J.C., Fernandez, M., Ranalli, G., Griffin, W.L., Connolly, J.A.D., 2008. Integrated geophysical–petrological modeling of the lithosphere and sublithospheric upper mantle: methodology and applications. Geochemistry Geophysics Geosystems 9, Q05008. http://dx.doi.org/10.1029/2007GC001834.

Afonso, J.C., Fullea, J., Griffin, W.L., Yang, Y., Jones, A.G., Connolly, J.A.D., O'Reilly, S.Y., 2013a. 3D multi-observable probabilistic inversion for the compositional and thermal structure of the lithosphere and upper mantle. I: a priori petrological information and geophysical observables. Journal of Geophysical Research - Solid Earth 118 (5), 2586–2617. http://dx.doi.org/10.1002/jgrb.50124.

Afonso, J.C., Fullea, J., Yang, Y., Connolly, J.A.D., Jones, A.G., 2013b. 3D multi-observable probabilistic inversion for the compositional and thermal structure of the lithosphere and upper mantle. II: General methodology and resolution analysis. Journal of Geophysical Research 118 (4), 1650–1676. http://dx.doi.org/10.1002/jgrb.50123.

Al-Kindi, S., White, N., Sinha, M., England, R., Tiley, R., 2003. Crustal trace of a hot convective sheet. Geology 31 (3), 207–210.

Amaru, M.L., Spakman, W., Villasenor, A., Sandoval, S., Kissling, E., 2008. A new absolute arrival time data set for Europe. Geophysical Journal International 173 (2), 465–472.

Arrowsmith, S.J., Kendall, M., White, N., VanDecar, J.C., Booth, D.C., 2005. Seismic imaging of a hot upwelling beneath the British Isles. Geology 33 (5), 345–348.

Artemieva, I.M., 2006. Global 1 degrees × 1 degrees thermal model TC1 for the continental lithosphere: implications for lithosphere secular evolution. Tectonophysics 416 (1–4), 245–277.

Artemieva, I.M., 2009. The continental lithosphere: reconciling thermal, seismic, and petrologic data. Lithos 109 (1–2), 23–46.

Ayarza, P., Palomeras, I., Carbonell, R., Afonso, J.C., Simancas, F., 2010. A wide-angle upper mantle reflector in SW Iberia: some constraints on its nature. Physics of the Earth and Planetary Interiors 181 (3–4), 88–102.

Barton, K.J., Brock, A., Sides, A.D., 1989. Preliminary results from temperature, heat flow and heat production studies in Ireland. In: Louwrier, K., Staroste, E., Garnish, J.D., Karkoulias, V. (Eds.), European Geothermal Update, Proceedings of the Fourth International Seminar on the Results of EC Geothermal Energy Research, Held in Florence, 27–30 April, 1989, pp. 551–559.

Bastow, I.D., Stuart, G.W., Kendall, J.M., Ebinger, C.J., 2005. Upper-mantle seismic structure in a region of incipient continental breakup: northern Ethiopian rift. Geophysical Journal International 162 (2), 479–493.

Bastow, I.D., Nyblade, A.A., Stuart, G.W., Rooney, T.O., Benoit, M.H., 2008. Upper mantle seismic structure beneath the Ethiopian hot spot: rifting at the edge of the African low-velocity anomaly. Geochemistry Geophysics Geosystems 9.

Bodin, T., Sambridge, M., Tkalcic, H., Arroucau, P., Gallagher, K., Rawlinson, N., 2012. Transdimensional inversion of receiver functions and surface wave dispersion. Journal of Geophysical Research—Solid Earth 117.

Bott, M.H.P., Long, R.E., Green, A.S.P., Lewis, A.H.J., Sinha, M.C., Stevenson, D.L., 1985. Crustal structure south of the Iapetus Suture beneath Northern England. Nature 314 (6013), 724–727.

Bowin, C., 2000a. Mass anomalies and the structure of the Earth. Physics and Chemistry of the Earth Part a—Solid Earth and Geodesy 25 (4), 343–353.

Bowin, C., 2000b. Mass anomaly structure of the Earth. Reviews of Geophysics 38 (3), 355–387.

Brace, W.F., 1965. Some new measurements of linear compressibility of rocks. Journal of Geophysical Research 70 (2), 391–&.

Bradley, S.L., Milne, G.A., Shennan, I., Edwards, R., 2011. An improved glacial isostatic adjustment model for the British Isles. Journal of Quaternary Science 26 (5), 541–552.

Brocher, T.A., 2005. Empirical relations between elastic wavespeeds and density in the Earth's crust. Bulletin of the Seismological Society of America 95 (6), 2081–2092.

Brock, A., 1979. Geothermal energy in Ireland: a preliminary assessment with particular reference to "hot dry rock" possibilities. AGR. 1979, 79/1.

Brock, A., 1989. Heat flow measurements in Ireland. Tectonophysics 164, 231–236.

Brock, A., Barton, K.J., 1984. Equilibrium temperature and heat flow density measurements in Ireland. Final Report on Contract No. EG-A-1-022-EIR(H). AGR 84/1, EUR 9517, National University of Ireland Galway, and European Commission.

Brown, C., Whelan, J.P., 1995. Terrane boundaries in Ireland inferred from the Irish magnetotelluric profile and other geophysical data. Journal of the Geological Society 152, 523–534.

Cermak, V., Rybach, L., 1979. Terrestrial Heat Flow in Europe. Springer Verlag.

Chadwick, R.A., Pharoah, T.C., 1998. The seismic reflection Moho beneath the United Kingdom and adjacent areas. Tectonophysics 299 (4), 255–279.

Chew, D.M., Stillman, C.J., 2009. Late Caledonian orogeny and magmatism, In: H. C.H., Sanders, I.S. (Eds.), The Geology of Ireland, 2nd edition. Dunedin Academic Press, Edinburgh, pp. 143–173.

Christensen, M.I., Mooney, W.D., 1995. Seismic velocity structure and composition of the continental crust — a global view. Journal of Geophysical Research—Solid Earth 100 (B6), 9761–9788.

Clark, R.A., Stuart, G.W., 1981. Upper mantle structure of the British Isles from Rayleigh wave dispersion. Geophysical Journal of the Royal Astronomical Society 67 (1), 59–75.

Connolly, J.A.D., 2005. Computation of phase equilibria by linear programming: a tool for geodynamic modeling and its application to subduction zone decarbonation. Earth and Planetary Science Letters 236, 524–541.

Davis, M.W., White, N.J., Priestley, K.F., Baptie, B.J., Tilmann, F.J., 2012. Crustal structure of the British Isles and its epeirogenic consequences. Geophysical Journal International 190 (2), 705–725.

Do, V.C., Readman, P.W., O'Reilly, B.M., Landes, M., 2006. Shear-wave splitting observations across southwest Ireland. Geophysical Research Letters 33 (3), 4.

Donaldson, C.H., 1978. Petrology of uppermost upper mantle deduced from spinel-lherzolite and harzburgite nodules at Calton Hill, Derbyshire. Contributions to Mineralogy and Petrology 65 (4), 363–377.

Downes, H., Upton, B.G.J., Handisyde, E., Thirlwall, M.F., 2001. Geochemistry of mafic and ultramafic xenoliths from Fidra (Southern Uplands, Scotland): implications for lithospheric processes in Permo-Carboniferous times. Lithos 58 (3–4), 105–124.

Downing, R.A., Gray, D.A., 1986. Geothermal Energy — The Potential in the United Kingdom. EUR 9505.

Eaton, D.W., Darbyshire, F., Evans, R.L., Gruetter, H., Jones, A.G., Yuan, X., 2009. The elusive lithosphere–asthenosphere boundary (LAB) beneath cratons. Lithos 109 (1–2), 1–22.

Fasano, G., Vio, R., 1988. Fitting a straight line with errors on both coordinates. Newsletter of Working Group for Modern Astronomical Methodology 7, 2–7.

Foulger, G.R., Panza, G.F., Artemieva, I.M., Bastow, I.D., Cammarano, F., Evans, J.R., Hamilton, W.B., Julian, B.R., Lustrino, M., Thybo, H., Yanovskaya, T.B., 2013. Caveats on tomographic images. Terra Nova 25 (4), 259–281.

Fullea, J., Afonso, J.C., Connolly, J.A.D., Fernandez, M., Garcia-Castellanos, D., Zeyen, H., 2009. LitMod3D: an interactive 3-D software to model the thermal, compositional, density, seismological, and rheological structure of the lithosphere and sublithospheric upper mantle. Geochemistry Geophysics Geosystems 10, 21. http://dx.doi.org/10.1029/2009GC002391 (ISSN: 1525-2027) (Q08019).

Fullea, J., Muller, M.R., Jones, A.G., 2011. Electrical conductivity of continental lithospheric mantle from integrated geophysical and petrological modeling: application to the Kaapvaal Craton and Rehoboth Terrane, southern Africa. Journal of Geophysical Research — Solid Earth. American Geophysical Union 116, 32. http://dx.doi.org/10.1029/2011jb008544 (B10202).

Fullea, J., Muller, M.R., Jones, A.G., Afonso, J.C., 2014. The lithosphere-asthenosphere system beneath Ireland from integrated geophysical-petrological modeling - II: 3D thermal and compositional structure. Lithos 189, 49–64 (this issue).

Gallagher, S., Elsdon, R., 1990. Spinel lherzolite and other xenoliths from a dolerite dyke in southwest Donegal. Geological Magazine 122, 177–180.

Giese, P., Scheuber, E., Schilling, F., Schmitz, M., Wigger, P., 1999. Crustal thickening processes in the Central Andes and the different natures of the Moho-discontinuity. Journal of South American Earth Sciences 12 (2), 201–220.

Goodman, R., Jones, G.L., Kelly, J., Slowey, E., O'Neill, N., 2004. Geothermal Energy Resource Map of Ireland (Dublin, Ireland).

Griffin, W.L., O'Reilly, S.Y., Ryan, C.G., 1999. The composition and origin of sub-continental lithospheric mantle. In: Fei, Y., Berkta, C.M., Mysen, B.O. (Eds.), Mantle Petrology: Field Observations and High-pressure Experimentation: A Tribute to Francis R. (Joe) Boyd. Spec. Publ. Geochem. Soc. , pp. 13–45.

Gunn, D.A., Jones, L.D., M.G., R., D.C., E., P.R.N., H., 2005. Laboratory measurement and correction of thermal properties for application to rock mass. Geotechnical and Geological Engineering 23, 773–791.

Hamza, V.M., Vieira, F.P., 2012. Global distribution of the lithosphere–asthenosphere boundary: a new look. Solid Earth 3 (2), 199–212.

Hauser, F., O'Reilly, B.M., Readman, P.W., Daly, J.S., Van den Berg, R., 2008. Constraints on crustal structure and composition within a continental suture zone in the Irish Caledonides from shear wave wide-angle reflection data and lower crustal xenoliths. Geophysical Journal International 175 (3), 1254–1272.

Holland, T.J.B., Powell, R., 1998. An internally consistent thermodynamic data set for phases of petrological interest. Journal of Metamorphic Geology 16 (3), 309–343.

Huber, P.J., 1981. Robust Statistics. John Wiley, New York (308 pp.).

Jacob, A.W.B., Kaminski, W., Murphy, T., Phillips, W.E.A., Prodehl, C., 1985. A crustal model for a northeast southwest profile through Ireland. Tectonophysics 113 (1–2), 75–103.

Janik, T., Grad, M., Guterch, A., Grp, C.W., 2009. Seismic structure of the lithosphere between the East European Craton and the Carpathians from the net of CELEBRATION 2000 profiles in SE Poland. Geological Quarterly 53 (1), 141–156.

Jones, A.G., Plomerova, J., Korja, T., Sodoudi, F., Spakman, W., 2010. Europe from the bottom up: a statistical examination of the central and northern European lithosphere–asthenosphere boundary from comparing seismological and electromagnetic observations. Lithos 120 (1–2), 14–29.

Julia, J., Ammon, C.J., Herrmann, R.B., Correig, A.M., 2000. Joint inversion of receiver function and surface wave dispersion observations. Geophysical Journal International 143 (1), 99–112.

Kelly, A., England, R.W., Maguire, P.K.H., 2007. A crustal seismic velocity model for the UK, Ireland and surrounding seas. Geophysical Journal International 171 (3), 1172–1184.

Khan, A., Connolly, J.A.D., Olsen, N., 2006. Constraining the composition and thermal state of the mantle beneath Europe from inversion of long-period electromagnetic sounding data. Journal of Geophysical Research—Solid Earth 111 (B10), 17.

Khan, A., Connolly, J.A.D., Taylor, S.R., 2008. Inversion of seismic and geodetic data for the major element chemistry and temperature of the Earth's mantle. Journal of Geophysical Research 113 (B09308).

Khan, A., Boschi, L., Connolly, J.A.D., 2009. On mantle chemical and thermal heterogeneities and anisotropy as mapped by inversion of global surface wave data. Journal of Geophysical Research—Solid Earth 114.

Khan, A., Zunino, A., Deschamps, F., 2011. The thermo-chemical and physical structure beneath the North American continent from Bayesian inversion of surface-wave phase velocities. Journal of Geophysical Research—Solid Earth 116.

Kind, R., Yuan, X.H., Kumar, P., 2012. Seismic receiver functions and the lithosphere–asthenosphere boundary. Tectonophysics 536, 25–43.

Kirstein, L.A., Timmerman, M.J., 2000. Evidence of the proto-Iceland plume in northwestern Ireland at 42 Ma from helium isotopes. Journal of the Geological Society 157, 923–927.

Kozlovskaya, E., Kosarev, G., Aleshin, I., Riznichenko, O., Sanina, I., 2008. Structure and composition of the crust and upper mantle of the Archean–Proterozoic boundary in the Fennoscandian shield obtained by joint inversion of receiver function and surface wave phase velocity of recording of the SVEKALAPKO array. Geophysical Journal International 175 (1), 135–152.

Kukkonen, I.T., Jokinen, J., Seipold, U., 1999. Temperature and pressure dependencies of thermal transport properties of rocks: implications for uncertainties in thermal lithosphere models and new laboratory measurements of high-grade rocks in the central Fennoscandian Shield. Surveys in Geophysics 20 (1), 33–59.

Landes, M., Prodehl, C., Hauser, F., Jacob, A.W.B., Vermeulen, N.J., 2000. VARNET-96: influence of the Variscan and Caledonian orogenies on crustal structure in SW Ireland. Geophysical Journal International 140 (3), 660–676.

Landes, M., O'Reilly, B.M., Readman, P.W., Shannon, P.M., Prodehl, C., 2003. VARNET-96: three-dimensional upper crustal velocity structure of SW Ireland. Geophysical Journal International 153 (2), 424–442.

Landes, M., Ritter, J.R.R., Readman, P.W., O'Reilly, B.M., 2005. A review of the Irish crustal structure and signatures from the Caledonian and Variscan orogenies. Terra Nova 17 (2), 111–120.

Landes, M., Ritter, J.R.R., O'Reilly, B.M., Readman, P.W., Do, V.C., 2006. A N–S receiver function profile across the Variscides and Caledonides in SW Ireland. Geophysical Journal International 165 (1), 814–824.

Landes, M., Ritter, J.R.R., Readman, P.W., 2007. Proto-Iceland plume caused thinning of Irish lithosphere. Earth and Planetary Science Letters 255 (1–2), 32–40.

Li, Y.H., Wu, Q.J., Zhang, R.Q., Tian, X.B., Zeng, R.S., 2008. The crust and upper mantle structure beneath Yunnan from joint inversion of receiver functions and Rayleigh wave dispersion data. Physics of the Earth and Planetary Interiors 170 (1–2), 134–146.

Licciardi, A., Lebedev, S., Piana Agostinetti, N., 2013. Imaging Ireland's crust with teleseismic receiver functions, with applications to geothermal research. Irish Geological Research Meeting, Derry, Northern Ireland.

Lowe, C., Jacob, A.W.B., 1989. A north–south seismic profile across the Caledonian Suture Zone in Ireland. Tectonophysics 168 (4), 297–318.

Masson, F., Jacob, A.W.B., Prodehl, C., Readman, P.W., Shannon, P.M., Schulze, A., Enderle, U., 1998. A wide-angle seismic traverse through the Variscan of southwest Ireland. Geophysical Journal International 134 (3), 689–705.

Masson, F., Hauser, F., Jacob, A.W.B., 1999. The lithospheric trace of the Iapetus Suture in SW Ireland from teleseismic data. Tectonophysics 302 (1–2), 83–98.

McDonough, W.F., Sun, S.S., 1995. The composition of the Earth. Chemical Geology 120 (3–4), 223–253.

Moorkamp, M., Jones, A.G., Eaton, D.W., 2007. Joint inversion of teleseismic receiver functions and magnetotelluric data using a genetic algorithm: are seismic velocities and electrical conductivities compatible? Geophysical Research Letters 34 (16).

Moorkamp, M., Jones, A.G., Fishwick, S., 2010. Joint inversion of receiver functions, surface wave dispersion, and magnetotelluric data. Journal of Geophysical Research—Solid Earth 115.

O'Donnell, J.P., Daly, E., Tiberi, C., Bastow, I.D., O'Reilly, B.M., Readman, P.W., Hauser, F., 2011. Lithosphere–asthenosphere interaction beneath Ireland from joint inversion of teleseismic P-wave delay times and GRACE gravity. Geophysical Journal International 184 (3), 1379–1396.

O'Reilly, B.M., Hauser, F., Readman, P.W., 2010. The fine-scale structure of upper continental lithosphere from seismic waveform methods: insights into Phanerozoic crustal formation processes. Geophysical Journal International 180 (1), 101–124.

O'Reilly, B.M., Hauser, F., Readman, P.W., 2012. The fine-scale seismic structure of the upper lithosphere within accreted Caledonian lithosphere: implications for the origins of the 'newer granites'. Journal of the Geological Society 169 (5), 561–573.

Pavlis, N.K., Holmes, S.A., Kenyon, S.C., Factor, J.K., 2008. An Earth Gravitational Model to Degree 2160: EGM 2008, European Geosciences Union. GRACE Science Applications, Session G3, Vienna, Austria.

Polat, G., Lebedev, S., Readman, P.W., O'Reilly, B.M., Hauser, F., 2012. Anisotropic Rayleigh-wave tomography of Ireland's crust: implications for crustal accretion and evolution within the Caledonian orogen. Geophysical Research Letters 39.

Poupinet, G., 1979. Relation between P-wave travel time residuals and the age of continental plates. Earth and Planetary Science Letters 43 (1), 149–161.

Poupinet, G., Arndt, N., Vacher, P., 2003. Seismic tomography beneath stable tectonic regions and the origin and composition of the continental lithospheric mantle. Earth and Planetary Science Letters 212 (1–2), 89–101.

Rao, C.K., Jones, A.G., Moorkamp, M., 2007. The geometry of the Iapetus Suture Zone in central Ireland deduced from a magnetotelluric study. Physics of the Earth and Planetary Interiors 161 (1–2), 134–141.

Readman, P.W., Oreilly, B.M., Murphy, T., 1997. Gravity gradients and upper-crustal tectonic fabrics, Ireland. Journal of the Geological Society 154, 817–828.

Robinson, J.A.C., Wood, B.J., 1998. The depth of the spinel to garnet transition at the peridotite solidus. Earth and Planetary Science Letters 164 (1–2), 277–284.

Rollin, K.E., 1995. A simple heat-flow quality function and appraisal of heat-flow measurements and heat-flow estimates from the UK geothermal catalog. Tectonophysics 244 (1–3), 185–196.

Roux, E., Moorkamp, M., Jones, A.G., Bischoff, M., Endrun, B., Lebedev, S., Meier, T., 2011. Joint inversion of long-period magnetotelluric data and surface-wave dispersion curves for anisotropic structure: application to data from Central Germany. Geophysical Research Letters 38.

Rychert, C.A., Shearer, P.M., 2009. A global view of the lithosphere–asthenosphere boundary. Science 324 (5926), 495–498.

Seipold, U., 1992. Depth dependence of thermal transport—properties for typical crustal rocks. Physics of the Earth and Planetary Interiors 69 (3–4), 299–303.

Seipold, U., 1995. The variation of thermal transport properties in the Earths crust. Journal of Geodynamics 20 (2), 145–154.

Shaw, C.S.J., Edgar, A.D., 1997. Post-entrainment mineral–melt reactions in spinel peridotite xenoliths from Inver, Donegal, Ireland. Geological Magazine 134 (6), 771–779.

Shen, W.S., Ritzwoller, M.H., Schulte-Pelkum, V., Lin, F.C., 2013. Joint inversion of surface wave dispersion and receiver functions: a Bayesian Monte-Carlo approach. Geophysical Journal International 192 (2), 807–836.

Sosa, A., Velasco, A.A., Velazquez, L., Argaez, M., Romero, R., 2013. Constrained optimization framework for joint inversion of geophysical data sets. Geophysical Journal International 193, 1745–1762. http://dx.doi.org/10.1093/gji/ggt326.

Su, B.X., Zhang, H.F., Asamoah, S.P., Qin, K.Z., Tang, Y.J., Ying, J.F., Xiao, Y., 2010. Garnet–spinel transition in the upper mantle: review and interpretation. Journal of Earth Science 21 (5), 635–640.

Tesauro, M., Kaban, M.K., Cloetingh, S., 2009. A new thermal and rheological model of the European lithosphere. Tectonophysics 476 (3–4), 478–495.

Upton, B.G.J., Downes, H., Kirstein, L.A., Bonadiman, C., Hill, P.G., Ntaflos, T., 2011. The lithospheric mantle and lower crust–mantle relationships under Scotland: a xenolithic perspective. Journal of the Geological Society 168 (4), 873–885.

van den Berg, R., Daly, J.S., Salisbury, M.H., 2005. Seismic velocities of granulite-facies xenoliths from Central Ireland: implications for lower crustal composition and anisotropy. Tectonophysics 407 (1–2), 81–99.

Vila, M., Fernandez, M., Jimenez-Munt, I., 2010. Radiogenic heat production variability of some common lithological groups and its significance to lithospheric thermal modeling. Tectonophysics 490 (3–4), 152–164.

Vosteen, H.D., Schellschmidt, R., 2003. Influence of temperature on thermal conductivity, thermal capacity and thermal diffusivity for different types of rock. Physics and Chemistry of the Earth 28 (9–11), 499–509.

Wawerzinek, B., Ritter, J.R.R., Jordan, M., Landes, M., 2008. An upper-mantle upwelling underneath Ireland revealed from non-linear tomography. Geophysical Journal International 175 (1), 253–268.

Wessel, P., Smith, W.H.F., 1998. New, improved version of the Generic Mapping Tools released. EOS Transactions AGU 79, 579.

Whelan, J.P., Brown, C., Hutton, V.R.S., Dawes, G.J.K., 1990. A geoelectric section across Ireland from magnetotelluric soundings. Physics of the Earth and Planetary Interiors 60 (1–3), 138–146.

Wilson, J.T., 1966. Did the Atlantic close and then re-open. Nature 211 (5050), 676-&.

York, D., 1966. Least-squares fitting of a straight line. Canadian Journal of Physics 44 (5), 1079–1086.

York, D., 1969. Least squares fitting of a straight line with correlated errors. Earth and Planetary Science Letters 5, 320–324.